

Synthesis, Characterization, *In vivo*, Molecular Docking, ADMET and HOMO-LUMO study of Juvenile Hormone Analogues having sulfonamide feature as an Insect Growth Regulators

Priyanka Sharma, Pamita Awasthi*

Department of Chemistry, National Institute of Technology, Hamirpur, H.P.-17 7005



ARTICLE INFO

Article history:

Received 26 February 2020

Revised 30 November 2020

Accepted 11 January 2021

Available online 20 January 2021

Keywords:

Juvenile Hormone (JH)

Juvenile Hormone Analogues (JHAs)

Insect growth regulators (IGRs)

Juvenile hormone binding proteins (JHBPs)

Docking

Galleria mellonella

larval mortality

lethal concentration (LC)

ADMET (Absorption, Distribution,

Metabolism, Excretion, and Toxicity)

HOMO-LUMO

ABSTRACT

The search for a simple and efficient method for the synthesis of sulfonamide derivatives as an Insect Growth Regulators (IGRs) under mild and eco-friendly conditions is of our interest. Here, we report a simple, efficient, and eco-friendly method for the synthesis of sulfonamide derivatives. A series of sulfonamides containing aniline derivatives have been synthesized. L-amino acid has been added in the intermediate steps which increase the bioactivity of the synthesized analogs. The structure elucidations of the synthesized analogs have been done using spectroscopic tools like - FTIR, NMR-¹H, ¹³C, ESI-MS. *In vivo* efficacy of the synthesized analogs has been investigated under laboratory conditions. *Galleria mellonella* has been chosen as a model insect, commonly known as honeycomb pest. *G. mellonella* causes a huge loss to beekeeping industries. All synthesized analogs showed insect growth regulatory action against the model species. Calculated LC₅₀ and LC₉₀ of all the analogs (T₁-T₈) against the fourth instar larvae were 9.99, 10.12, 13.70, 13.59, 13.94, 21.69, 13.28, 12.80 ppm and 153.27, 131.69, 113.23, 161.70, 141.48, 205.75, 110.93, 96.91 ppm, respectively. Among these analogs, N-(1-isopropyl-2-oxo-2-p-nitroanilino-ethyl) toluene-p-sulphonamide (T₈) and N-(1-isopropyl-2-oxo-2-p-nitroanilino-ethyl) benzene-sulphonamide (T₇) exhibited the good pest larval mortality in comparison to in use IGR like- Pyriproxyfen (T₁) and Fenoxycarb (T₂). Docking using AutoDock 4.2 has been carried out to identify the potential binding affinities and mode of interaction of the synthesized analogs (T₃-T₈) with Juvenile Hormone Binding Protein (JHBP) of *G. mellonella* in comparison to in use IGRs Pyriproxyfen (T₁) and Fenoxycarb (T₂). Additionally, *in silico* ADMET (absorption, distribution, metabolism, excretion, and toxicity) filtration has been used to predict the properties of the analogs. Quantum chemical calculations like Density Functional Theory have been performed to calculate different global reactivity descriptors. A small difference between HOMO and LUMO energy signifies the electronic excitation energy which is essential to calculate molecular reactivity and stability of the aniline based sulfonamides (T₃-T₈).

© 2021 Elsevier B.V. All rights reserved.

Introduction

The overuse of conventional pesticides/Insecticides has caused a major threat to an environment. The use of these chemicals has created an imbalance in the ecosystems. Insects have developed resistance against them and soil has lost fertility. Need has been felt by the chemist worldwide to look for safer alternatives. Insect growth regulators (IGRs) are considered to be third generation pesticides and have the potential to replace the conventional pesticides/Insecticides from the market. These IGRs are safer to use, species-specific, target in action, biodegradable, environment-friendly, and non-toxic to humans. This class of chemicals has

been categorized into a) terpenoid b) non-terpenoid series of compounds. The non-terpenoid Phenoxy derivatives were found to be more bioactive against different insect pest species [54].

Insects have a very fast multiplication rate. Sudden arrest in insect and pest populations may cause an imbalance in the ecosystem by affecting directly/indirectly processes like food web, food chain, pollination, etc. Therefore, it is advisable to control insect and pest populations slowly and steadily without disturbing the ecosystem [61]. Insect species exhibit a distinct phenomenon of metamorphosis (Egg-Larva-Pupa-Adult). This process is under the control of two important hormones that are released by the endocrine system of the insects namely -Juvenile Hormone & Ecdysteroid Hormone. A slight variation in the amount and secretion of these hormones results in the physical deformities in insect species which result in reduced population growth [49,61]. Juve-

* Corresponding author.

E-mail addresses: pamita@nith.ac.in, pamitawasthi@gmail.com (P. Awasthi).

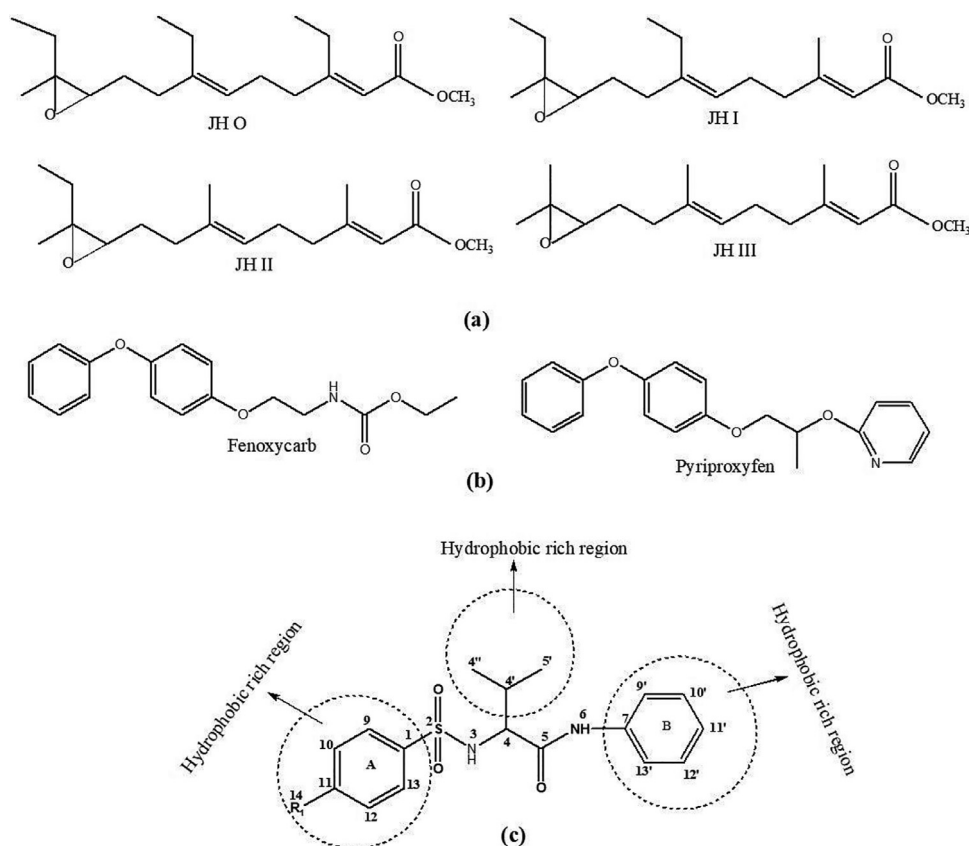


Fig. 1. (a) Natural Juvenile Hormones; (b) Synthetic Insect Growth Regulators (T₁-T₂); (c) Structure of parent analog of synthesized series (T₃-T₈).

nile Hormone after release from the endocrine system combined with carrier proteins present in the hemolymph (Fig. 1a). These carrier proteins have a strong binding affinity and stereoselectivity for JH molecules [14,32,45,33] and known as Juvenile Hormone Binding Proteins (JHBPs). JHBPs undergo a profound conformational transition upon binding to JH [79]. Juvenile hormone analogs (JHAs) are believed to be JH mimics. JHA's are proposed to act by interacting with various proteins present in the hemolymph [47,46,77,69,67,30]. JH analogs are reported to keep the insects in an immature and potentially injurious stage longer than normal time and ultimately affect insect population.

Among all synthetic IGR's, Pyriproxyfen (Pyridine based IGR) showed highly inhibitory reproductive and metamorphic action against agricultural, household, and public hygiene insects and pests. It is effective against mosquitoes, Sunn pest (*Eurygaster integriceps Puton*), onion thrips (*Thripstabaci Lindeman*), the mealworm (*Tenebrio molitor*), house flies (*Musca domestica*), etc. It has been proposed to exhibit low mammalian toxicity. The mode of action, as well as the environmental behavior of Pyriproxyfen completely differs from organo-chlorinated and organo-phosphorous compounds (Fig. 1b) [4,37,44,3,11]. In the present study, Pyriproxyfen (T₁) is chosen as the standard. It is an important IGR against *Galleria mellonella* as it causes physiological and pathological changes in *G. mellonella* hemocytes. The toxic effect of Pyriproxyfen on endocrine glands resulted in the reduction of total hemocyte count which is due to the clumping of hemocytes. Pyriproxyfen also causes damage to the plasma membrane of hemocytes of *Galleria mellonella*. A combination of Pyriproxyfen and *B. thuringiensis* affected the antioxidant defense system of *G. mellonella* larvae even at low doses [64,65]. Fenoxycarb (T₂), a carbamate feature containing the class of IGR, exhibits ovicidal activity. It is effective against flea, mosquito, and cockroach control. It is also used in an inte-

grated pest management program. Further, Fenoxycarb is mainly used to control Lepidoptera species in fruit orchards and vineyards [12,34,51]. Fenoxycarb (T₂) also finds its applications to control the population of *G. mellonella* as it altered male gonad physiology, causing germ cell death at different stages of differentiation. Treatment of *G. mellonella* larvae with Fenoxycarb resulted in larval diapause, mainly immediately after its application [10]. Several JHAs with different structural features have been reported in the literature and exhibited antagonist effect against most of the harmful insect species [6,29,36,43,48,54,68,76,75].

The greater wax moth, *Galleria mellonella* Linnaeus, is a ubiquitous pest of the honeybee mainly *Apis mellifera* and *Apis cerana* worldwide. *G. mellonella* causes the greatest damage in apiaries which leads to huge financial losses every year. Almost all the colonies of Asian honeybees are prone to moth infestation. Wax moth belongs to the subfamily Galleriinae of the family Pyralidae, order Lepidoptera. Wax moth infestation is at its peak during the monsoon season from July to August during summer and December to January during the winter season [13,50]. Therefore, there is a need for more studies to find sustainable integrated pest management strategies. The population of *G. mellonella* can be controlled by biological and chemical methods. The successful and sustainable biological control agent for *G. mellonella* is still lacking. Chemical control involved the use of fumigants in most beekeeping regions. Various types of fumigants have been used and found to be effective against wax moth include sulfur, acetic acid, ethylene bromide, calcium cyanide, phosphine, paradichlorobenzene (PDB), naphthalene, and carbon dioxide. More importantly, they are poisonous to honeybee colonies and non-target species [58,74,16].

Sulfonamides, the most common scaffolds in sulfur-containing molecules, are well studied in synthesis and application during the past decades, is the subject of our interest. Sulfur-containing com-

pounds have shown diverse biological activity and serve an important function in the pharmaceutical industry [27]. Sulfur is considered to be a general-use pesticide in agriculture. Benzene sulfonamides with low cost and low toxicity are popularly used as insecticide/Pesticide in the agrochemical field [21,63,71]. The presence of a nucleophilic group on this compound allows further chemical modifications to obtain novel sulfonamide derivatives. A variety of aniline derivatives as a nucleophilic agent are allowed to react with benzene sulfonamide carboxylic acid chlorides to obtain a new series of analogs. Aniline and its derivatives find vast application in drugs, pesticides, rubber azo dyes photographic chemicals, etc. [70,39]. Four analogs were further modified by replacing Hydrogen atom at position 11' with chlorine or nitro group in the aryl ring B (Fig. 1c). The nitro group/chloro group with various electronic properties and spatial characteristics were considered to explore the relationship between structure and pesticide activity. The results indicate that the electron-withdrawing group at position 11' on the aryl ring B plays a unique role in enhancing the pesticide activity [35,39,42,18,78].

The work presented here is a part of the pest management program carried out in our laboratory. In this paper, we report synthesis, characterization, *in vivo* testing, Docking, ADMET, and HOMO-LUMO study of JHAs having sulfur group, L-amino acid, and aniline derivative having lipophilic group along with hydrophobic terminations at the ends of the main chain with JHBP of *G. mellonella* (Fig. 1c).

Materials and Methods

2.1. General methods and material for the synthesis

Chemical reagents and solvents used were purchased from Sigma Aldrich of 99% purity grade.

Analog (T₃-T₈) have been synthesized in our laboratory using a simple reaction scheme (Fig. 2). The progress of the reaction was monitored by thin-layer chromatography (TLC).

The following solvent systems were employed – a. Benzene: Methanol (8:2), b. Ether: Pet-Ether: Ethyl acetate (5:5:2).

Melting points were determined on a hot-stage apparatus and are uncorrected. Each compound was synthesized and verified by spectroscopic methods. FT-IR spectra were recorded on Perkin Elmer 1600 spectrophotometer with the samples as compressed KBr pellets ranging from 4000 to 400 cm⁻¹. ¹H and ¹³C NMR spectra were recorded using a Bruker Avance 400 MHz spectrophotometer operating at room temperature in DMSO d₆ as the solvent. The electron spray ionization-mass spectroscopy (ESI-MS) analyses were carried out in positive ion modes using a Water Q of Micro-mass.

2.2. Rearing of the insect model

An artificial diet has been developed for mass rearing of *Galleria mellonella* in our laboratory (temperature 27±1°C, relative humidity 65±5 % and 16:8 hr scoto-photo-phase regime) and prepared by a well-defined method with some modifications [5].

In vivo efficacy of Analogs (T₁-T₈) as IGRs

A laboratory-reared colony of *G. mellonella* larvae was used for IGR activity. Ten larvae of fourth instars were kept in a 500 ml glass beaker. The diverse concentration of all analogs (T₁-T₈) ranging from 10 ppm to 100 ppm, in acetone on w/v basis, has been used for testing against lepidopteran insect species to show IGR effects. The control mortalities were corrected by using Abbott's

formula [1].

Corrected mortality =

$$\frac{\text{Observed mortality in treatment} - \text{observed mortality in control}}{100 - \text{Control mortality}} \times 100$$

$$\text{Percentage mortality} = \frac{\text{Number of dead larvae}}{\text{Number of larvae introduced}} \times 100$$

The LC₅₀ and LC₉₀ were calculated from toxicity data using probit analysis [28].

2.2.2. Efficacy of Analogs (T₁-T₈) for anti-Juvenile hormone activity (Pesticidal action)

When the pest crop is on full destruction to the host; the need is felt for the immediate action of in use IGRs. The diverse concentration of these in use IGRs; Pyriproxyfen (T₁) and Fenoxycarb (T₂) ranging from 1000 ppm to 10,000 ppm, in acetone on a w/v basis, has been used for testing against lepidopteran insect species to show pesticidal effects [3,25,31,52].

Larvae of the fourth instar of *G. mellonella* were collected and maintained for the treatment. Acetone solution (2 ml) containing the analog was poured on the filter paper in each petri dish and allowed to evaporate. Later, the counted number of larvae to be treated was transferred to the Petri dishes and applying the different concentrations of the analogs to them. The mortality rate was noted for each of the replication sets. Each treatment involved three replicates with each replicate containing ten insects. The same procedure has been applied for all the analogs (T₁-T₈).

Different concentrations ranging from 250 ppm to 2000 ppm have been prepared to check the immediate action of all the synthesized analogs with a lesser exposure period (2-10 hours). Synthesized analogs (T₃-T₈) and in use IGRs (T₁ & T₂) did not show any visible change in the insect behavior up to 750 ppm for ten hours of exposure period but changes were seen at 1000 ppm from four hours to ten hours exposure period. 2 ml volume of each has been used for *in vivo* study.

2.2.3. Statistical analysis

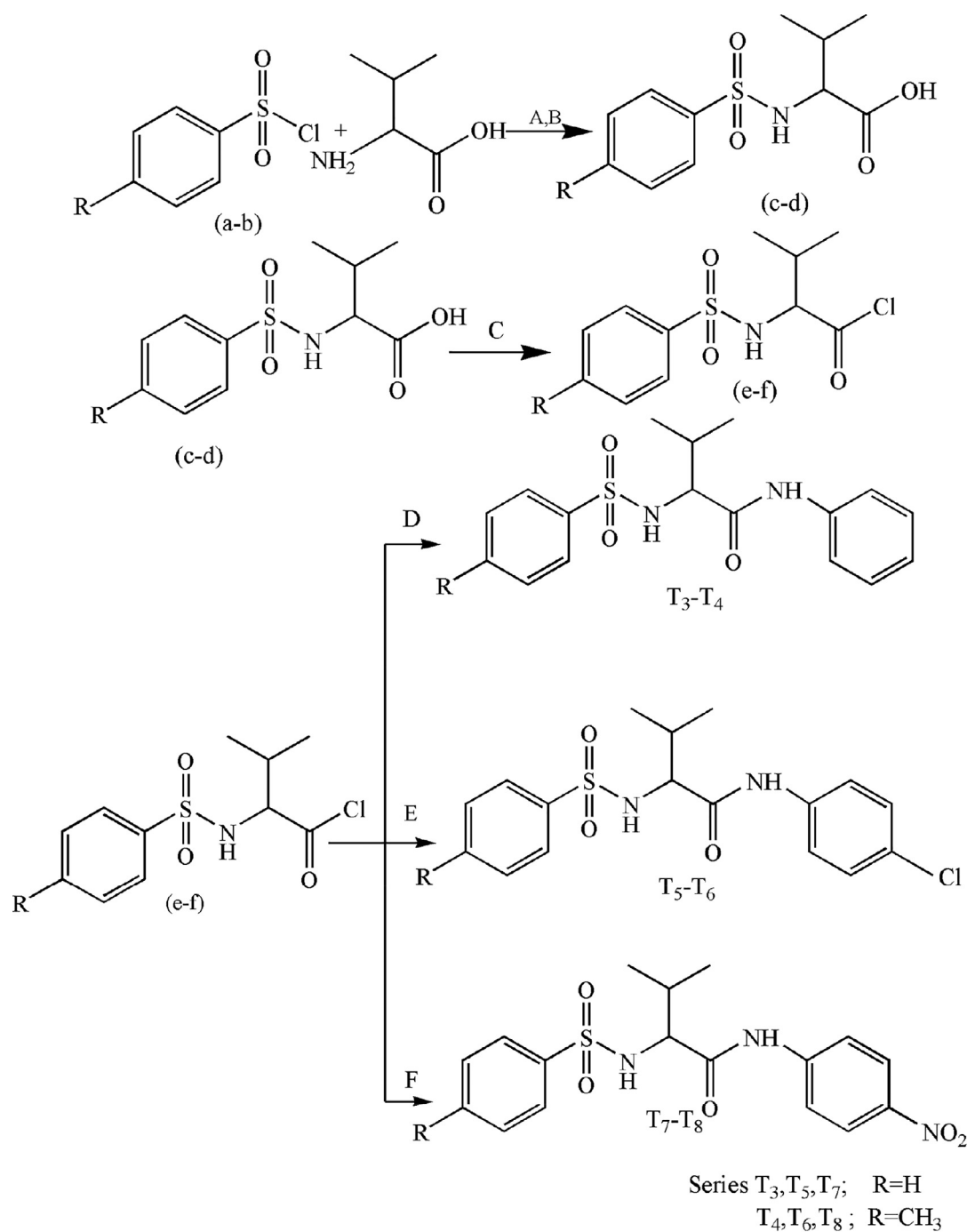
For IGR action the data were subjected to analysis of variance. The average larval mortality data were further subjected to probit analysis for calculating LC₅₀ and LC₉₀ values [28]. For pesticidal action, the data were grouped according to the number of analogs (T₁ to T₈), concentration (C in ppm), and exposure time (I in hours) and subjected to analysis of variance. Further data were statistically analyzed to calculate the critical difference (CD) at P ≤ 0.05.

2.3. Principle of Molecular docking using AutoDock 4.2

AutoDock 4.2 an automated docking tool (The Scripps Research Institute La Jolla, CA 92037-1000, U.S.A.) has been used for the present study to predict the mode of binding of JH Analogues to a receptor protein. The semiempirical force field evaluates binding in two steps. In the first step, intramolecular energetics is estimated for the transition from unbound states to the bound state whereas the second step evaluates the intermolecular energetics of combining the ligand and protein in their bound conformation. The force field includes six pair-wise evaluations (V) and estimates the conformational entropy lost upon binding (ΔS_{conf}):

$$\Delta G = (V_{bound}^{L-L} - V_{unbound}^{L-L}) + (V_{bound}^{P-P} - V_{unbound}^{P-P}) + (V_{bound}^{P-L} - V_{unbound}^{P-L} - \Delta S_{conf})$$

(L refers to the "ligand" and P refers to the "protein" in a ligand-protein docking calculation) (<http://autodock.scripps.edu/>)



Reagent : (A) NaOH (B) HCl (C) SOCl₂
(D) NH₂-C₆H₅ (E) NH₂-C₆H₄-Cl (F) NH₂-C₆H₄-NO₂

Fig. 2. Complete synthesis of juvenile hormone analogs (T₃-T₈)

Further analogs are screened based upon their scoring function. In AutoDock the implemented scoring function is defined as an empirical binding free energy function. Each of the pair-wise energetic terms includes evaluations for dispersion/repulsion, hydrogen bonding as per the following expression:

$$\Delta G = \Delta G_{vdw} \sum_{i,j} \left(\frac{A_{ij}}{r_{ij}^{12}} - \frac{B_{ij}}{r_{ij}^6} \right) + \Delta G_{hbund} \sum_{i,j} E(\phi) \left(\frac{C_{ij}}{r_{ij}^{12}} - \frac{D_{ij}}{r_{ij}^{10}} \right) + \Delta G_{elec} \sum_{i,j} \frac{q_i q_j}{\epsilon(r_{ij}) r_{ij}} + \Delta G_{tor} N_{tor} + \Delta G_{sol} \sum_{i,j} (S_i V_j + S_j V_i) e^{(-r_{ij}^2/2\sigma^2)}$$

[ΔG =change in free energy; ΔG_{vdw} : 12-6 Lennard-Jones potential; ΔG_{ele} : Coulombic with Solmajer-dielectric; ΔG_{H-bond} : 12-10 Potential with Goodford Directionality; ΔG_{tors} : Number of rotatable bonds; ΔG_{sol} : Stouten Pairwise Atomic Solvation Parameters; ΔG_{tor} is a measure of the unfavorable entropy of ligand binding due to the restriction of conformational degrees of freedom, and N_{tor} is the number of sp³ bonds in the ligand].

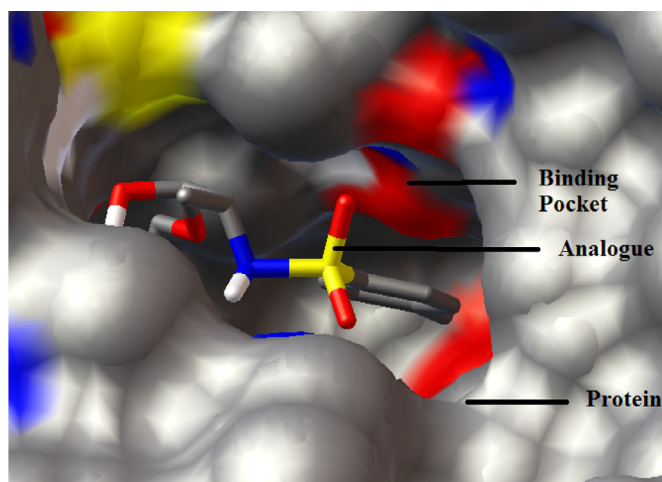


Fig. 3. Docked structure of JH Analogs inside the binding cavity of JH binding protein (PDB 2RCK) (structures have been drawn by using Auto Dock 4.2 software)

2.3.1. Preparation of files

The structures of JH analogs have been built using pymol software tool (www.pymol.com) and optimized using AMBER force field. Gasteiger charge has been assigned to ligands and then non-polar hydrogens were allowed to merge. The rigid roots were defined automatically for each compound. Further *Auto Tor* module has been applied to define the flexibility of the bonds in the ligands. Final ligand structures were saved as *ligand.pdbqt* format. The PDB file of the JHBP of *G. mellonella* (2RCK) has been downloaded from the protein data bank (www.rcsb.org). Polar hydrogens were added to the macromolecule (2RCK) using the ADDSOL utility of AutoDock 4.2. The Kollman charges were added to each atom of chain A and saved as *protein.pdbqt* format. A grid box was generated around the binding cavity of the JHBP by selecting key amino acid residues THR 22, TYR 128 & 130 [46] (Fig. 3). It was generated for the calculation of docking interaction energy followed by the generation of grid parameter file *pro.gpf* of protein using the Auto Grid Tool of the software. Since the structure of the protein kept rigid and known, interaction energies between the probe and surrounding amino acids have been calculated at each point in the grid and stored in the output file as *pro.glg*. The grids were chosen to be sufficiently large to include not only the active site but also a significant portion of the surrounding surface at receptor protein with grid points $69 \times 67 \times 69$, along with a grid spacing of 0.531 \AA . Lamarckian Genetic Algorithm (LGA) protocol has been used for protein fixed: ligand flexible model [63,38,53].

For the local search, the pseudo-solis and wets algorithm was applied. Other docking parameters were set as default. Final docking orientations lying within 2 \AA of the root-mean-square deviation (rmsd) tolerance of each other were represented as the most favorable conformation with the low free energy of binding (ΔG_b). The dock parameter file for ligand was saved as *lig.dpf*. All the analogs were ranked according to their binding free energy (ΔG_b in kcal/mol) and inhibition constant (K_i in μM) at 298.15K. Overall, the free energy of binding (ΔG_b) was composed of a sum of free energies measured for each analog pose and given as:

$$\Delta G_b = \text{IntermolecularEnergy} + \text{InternalEnergy} \\ + \text{Torsionalenergy} - \text{Unboundsystem'senergy}$$

$$\text{IntermolecularEnergy} = a\Delta G_{vdw} + b\Delta G_{ele} + c\Delta G_{H-bond} + e\Delta G_{sol}$$

(Since Auto Dock 4.2 measures the Final Total Internal Energy same as Unbound System's Energy and equal to the difference between the internal energy of the unbound model and the inter-

nal energy of the ligand when it is bound to the protein.) [<http://autodock.scripps.edu/>]

Therefore,

$$\Delta G_{bind} = a\Delta G_{vdw} + b\Delta G_{ele} + c\Delta G_{H-bond} + d\Delta G_{tors} + e\Delta G_{sol}$$

(Here ΔG =change in free energy; ΔG_{vdw} : 12-6 Lennard-Jones potential; ΔG_{ele} : Coulombic with Solmajer-dielectric; ΔG_{H-bond} : 12-10 Potential with Goodford Directionality; ΔG_{tors} : Number of rotatable bonds; ΔG_{sol} : Stouten Pairwise Atomic Solvation Parameters; a, b, c, d and e terms are scaling coefficient obtained using AutoDock force field and by default, their values are: $\Delta G_{bind} = 0.1662vdw + 0.1406 ele + 0.1209 H-bond + 0.2983tors + 0.1322desolve$)

$$K_i = \exp((\Delta G \times 1000)/(R \times T))$$

(Where ΔG_b is binding energy, $R = 1.98719 \text{ cal}$ and $T = 298.15$ (temp in Kelvin))

A combination of intermolecular + internal energy is measured as 'dock energy', while intermolecular + torsional energy is measured as 'binding energy'. The same protocol was applied for all analogs (T_3 - T_8) and standard IGR's (pyriproxyfen and fenoxycarb).

All simulations have been performed on the Linux operating system with system Properties (Intel(R) Pentium(R) D CPU 2.80GHz, 4.0 GB of RAM).

In silico ADMET screening

Absorption, distribution, metabolism, elimination, and toxicity (ADMET) properties were analyzed using ADMET descriptors on Discovery Studio 2.1. It has six mathematical models to quantitatively predict the properties like - ADMET absorption level (human intestinal absorption); ADMET aqueous solubility level; ADMET BBB (Blood Brain Barrier penetration level); ADMET CYP2D6 (Cytochrome P450 2D6 enzyme inhibition); ADMET hepatotoxicity; ADMET PPB (plasma protein binding level) (Table 1).

These properties indicate threshold ADMET characteristics for the chemical structure of synthesized JH analogs (T_3 - T_8) and Synthetic IGRs (T_1 - T_2). All synthesized compounds were subjected to ADMET study to predict the level of toxicity and side effects on humans.

AlogP (ADMET AlogP98) and 2D polar surface area (ADMET PSA_2D) calculations in ADMET can predict human intestinal absorption (HIA). The absorption level of the HIA model is defined by 95% and 99% confidence ellipses by plotting ADMET AlogP98 vs ADMET PSA_2D [15,17,22,66,23,19].

Quantum chemical studies: The quantum chemical calculations were carried out on Gaussian 98 software. Structures were visualized in Gaussview 3.0 software tool. All the analogs (T_1 - T_8) were fully optimized using the B3LYP/6-31+G (d, p) level of basis set using the Density Functional Theory method. After optimizations of analogs, energies of the highest occupied molecular orbital (HOMO) and lowest unoccupied molecular orbital (LUMO) were obtained from occupied and virtual eigenvalues mentioned in the Gaussian output file. Further, the reactivity descriptors such as energy gap, electrophilicity index, chemical hardness, and softness, etc. have been calculated from HOMO -LUMO data [72,55,56]. The present work examines the applicability of all chemical descriptors in the prediction of biological activity of a class of synthesized JH analogs (T_3 - T_8) to be potential insect growth regulators (IGRs).

Results and Discussion

3.1. Synthesis of N-(1-isopropyl-2-oxo-2-anilino-ethyl) benzene sulfonamide and related compounds (T_3 - T_8)

Synthesis of N-(1-isopropyl-2-oxo-2-anilino-ethyl) benzene sulfonamide and related compounds (T_3 - T_8) has been achieved by the

Table 1
ADMET descriptors and their rules/keys [57].

ADMET absorption level (human intestinal absorption)	
Level	Description
0	Good absorption
1	Moderate absorption
2	Low absorption
3	Very low absorption
ADMET (blood brain barrier penetration level) BBB	
Level	Description
0	Very High
1	High
2	Medium
3	Low
4	Undefined
5	Molecules with one or more unknown Alog P calculation
ADMET CYP2D6	
Predicted Class	Value
0	Noninhibitor
1	Inhibitor
ADMET Hepatotoxicity	
Predicted Class	Value
0	Nontoxic
1	Toxic
ADMET (plasma protein binding level) PPB	
Level	Description
0	Binding is <90%
1	Binding is ≥ 90%
2	Binding is ≥ 95%
ADMET aqueous solubility level	
Level	Description
0	Extremely Low
1	No, very low, but possible
2	Yes, low
3	Yes, good
4	Yes, optimal
5	No, too soluble
6	Molecule with one or more unknown AlogP98 types.

action of substituted aniline with acid chlorides in dry benzene. N-(1-isopropyl-2-oxo-2-anilino-ethyl) benzene sulfonamide and related compounds (T₃-T₈) are new in literature and fully identified based on their spectral data (IR, ¹H NMR, ¹³C NMR, and ESI-MS analysis). All the compounds have been obtained as pure solids. (Supplementary Data)

3.2. Bioassay of synthesized analogs on *G. mellonella*

All the analogs have been screened for their IGRs and pesticidal action against fourth instar larvae of *Galleria mellonella* (Honeycomb pest). The population of ten larvae each in three replication sets has been studied for larval mortality at different concentrations (in ppm) having variable exposure periods (in hours). Table 2 provides the results of IGR action of all the synthesized analogs (T₃-T₈) along with in-use IGRs (T₁ and T₂) during the treatment of fourth instar larvae of *G. mellonella* (wax moth) at different concentrations (10-100 ppm) at different exposure period (12 hrs.-72 hrs.). The highest mortality rate has been observed at 72 hours of exposure time. LC₅₀ value for all the synthesized analogs falls in the range of 12.80 to 21.69 ppm in comparison to commercially in use IGRs like Pyriproxyfen (T₁) and Fenoxycarb (T₂) having LC₅₀ value 9.99 and 10.12 ppm respectively. Synthesized analogs like T₃, T₄, T₅, T₇, and T₈ showed the LC₅₀ value (12.80-13.94 ppm) very close to in use IGRs (Fig. 4). The overall pattern of LC₅₀ for all the analogs in comparison to in use IGRs against fourth larval instar of *G. mellonella* was - T₁>T₂>T₈>T₇>T₄>T₅>T₃>T₆ and the pattern for LC₉₀ is T₈>T₇>T₂>T₅>T₁>T₄>T₃>T₆. Among the synthesized series (T₃-T₈), analog T₈ exhibited the highest mortality rate having LC₅₀ 12.80 ppm at concentrations ranging from 10 to 100 ppm after 72 hours of exposure time (Table 2 and Fig. 4). Further, the pesticidal action of all the analogs (T₁-T₈) has been studied

at higher concentrations ranging from 750 to 2000 ppm at different exposure time from 2 to 10 h. The mortality rate was insignificant at concentrations ranging from 250-750 ppm at a lesser exposure time (2-10 hours) in comparison to previous IGR studies [63]. The larval mortality of *G. mellonella* increased with an increase in the concentration of the different analogs-based formulations. A significantly progressive increase in mortality was recorded with the increase in the exposure period as well as concentration. All treatments showed maximum efficacy against *G. mellonella* at 2000 ppm after 10 hours of exposure time.

All the synthetic analogs (T₃-T₈) showed significant effects on larval mortality at 1000 ppm and 1500 ppm after 10 hours of exposure (Fig. 5). The observations regarding the effect of different concentrations (in ppm) of sulfonamide IGR's at different exposure periods (in hours) on percent larval mortality of *G. mellonella* have been tabulated in Table 3.

None of the treatments were significantly effective at 1000 ppm concentration after exposure of 2 hours. Although there was a progressive increase in mortality with an increase in the exposure period (Fig. 6a), the overall rate of mortality remained low at this concentration. T₁ and T₂ showed maximum efficacy of 100.00 % kills at 8 hours exposure period. T₆ and T₈ with the same concentration exhibit 90.00 and 93.33 % mortality at the exposure period of 8 hours, respectively. Mortality did not exceed 60.00 % in the rest of the treatments for the same exposure period. Increasing the exposure periods up to 10 hours, T₆ and T₈ attained the 100.00 % larval mortality followed by T₄ and T₇ at the same concentration. Mortality did not exceed 84.00 % in all other formulations. Trends were similar at 1500 ppm concentration. T₃ formulation was found to be least effective with 16.67 % kill at 2 hours exposure time while T₈ formulation at the same exposure period exhibited 56.67 % mortality (Fig. 6b). While percent mortality in T₈ enhanced from 56.67 to 100.00 % at 6 hours exposure period, T₂ showed the enhancement from 53.33 % to 100.00 % at 6 hours followed by T₁ from 46.67 % to 100.00 % mortality at similar exposure periods. T₆ also showed an increase from 26.67 % to 100.00 % kill. Likewise, T₇ exhibited the enhancement from 23.33 % to 100.00 % kill at a similar exposure period (6 hours) at the same concentration. In the case of T₄ formulation 90.00 %, larvae were killed when exposed to 1500 ppm for 6 hours. T₃ and T₅ were least effective registering 73.33 and 83.33 % mortality and these values were insignificant to each other (Table 3). The highest percent of larval mortality at 2000 ppm concentration up to 4 hours exposure was shown by T₁ (100.00 %), T₂ (100.00 %) followed by T₇ and T₈. Likewise, T₄, T₅, and T₆ also showed higher mortality of 93.33 % at the same exposure period of 4 hours at the same concentrations. Formulation T₃ showed the least 86.67 % mortality which is statistically insignificant to others (Fig. 6c). However, at 6 hours of exposure, the rest of the formulations showed the 100.00 % larval mortality. Overall, there occurred an increase in concentration and an increase in the exposure period. Clear morphological changes have been observed at the fourth larval instar of *G. mellonella* (Fig. 6(a-c)).

3.3. JHBP- JHAs Interactions

JHBP has been proposed to be the binding site of natural juvenile hormone. Detailed structural studies of JHBP of *G. mellonella* with JH-III has been solved [46]. In rational bioactive molecular design, an accurate estimate for the binding free energy is important to justify the difference in binding affinity between different JH analogs towards JH binding protein (JHBP). JHAs interactions with JHBP depends upon specific and non-specific forces present inside the binding pocket of the receptor protein. Electrostatic interactions of structurally diverse data sets including series of JH analogs vary mainly from each other by the number of C-atoms,

Table 2
Probit analysis of sulfonamide analogs for IGR action (T₁-T₈) against *G. mellonella*

S. No.	Analog	% Larval mortality					LC ₅₀ (ppm)	95% Confidence		LC ₉₀ (ppm)	95% Confidence		Regression Equation
		Conc (ppm)						Limits			Limits		
		10	25	35	50	100		LCL	UCL		LCL	UCL	
1.	T ₁	44	59	67	78	89	9.99	2.44	17.53	153.27	75.00	231.54	3.53+1.25X
2.	T ₂	46	61	68	79	89	10.12	3.69	16.54	131.69	73.22	190.17	3.52+1.30X
3.	T ₃	41	56	70	82	89	13.70	8.28	28.03	113.23	101.10	294.57	3.17+1.51X
4.	T ₄	41	56	67	74	85	13.59	5.17	22.01	161.70	83.68	239.73	3.38+1.30X
5.	T ₅	39	54	68	79	86	13.94	5.93	21.95	141.48	81.23	201.73	3.26+1.40X
6.	T ₆	32	50	57	68	82	21.69	9.83	33.38	205.75	102.99	308.51	3.12+1.36X
7.	T ₇	39	57	71	79	89	13.28	6.55	20.00	110.93	71.95	149.91	3.13+1.53X
8.	T ₈	39	57	75	82	89	12.80	6.67	18.93	96.91	66.12	127.70	3.08+1.60X

- 1 T₁: Pyriproxyfen (Standard); T₂: Fenoxycarb (Standard)
 2 T₃: N-(1-isopropyl-2-anilino-2-oxo-ethyl) benzene sulphonamide; T₄: N-(1-isopropyl-2-anilino-2-oxo-ethyl) toluene-p- sulphonamide
 3 T₅: N-(1-isopropyl-2- p-chloroanilino-2-oxo -ethyl) benzene-sulphonamides; T₆: N-(1-isopropyl-2- p-chloroanilino-2-oxo--ethyl) toluene-p-sulphonamides
 4 T₇: N-(1-isopropyl-2- p-nitroanilino-2-oxo -ethyl) benzene-sulphonamides; T₈: N-(1-isopropyl-2- p-nitroanilino-2-oxo ethyl) toluene-p-sulphonamides

Table 3
Effect of different concentrations of IGRs (T₁-T₂) and synthesized analogs (T₃-T₈) at different exposure periods on per cent larval mortality of *G. mellonella* (in vivo)

Formulations	Per cent larval mortality at concentration (ppm)														
	1000 ppm					1500 ppm					2000 ppm				
	Exposure period (hours)					Exposure period (hours)					Exposure period (hours)				
	2	4	6	8	10	2	4	6	8	10	2	4	6	8	10
T ₁	0.00 0.00*	56.67 48.93*	90.00 71.57*	100.00 90.00*	100.00 90.00*	46.67 43.08*	83.33 66.15*	100.00 90.00*	100.00 90.00*	100.00 90.00*	100.00 90.00*	100.00 90.00*	100.00 90.00*	100.00 90.00*	100.00 90.00*
T ₂	0.00 0.00*	43.33 41.16*	70.00 57.00*	100.00 90.00*	100.00 90.00*	53.33 46.92*	90.00 75.00*	100.00 90.00*	100.00 90.00*	100.00 90.00*	100.00 90.00*	100.00 90.00*	100.00 90.00*	100.00 90.00*	100.00 90.00*
T ₃	0.00 0.00*	10.00 18.44*	26.67 31.00*	40.00 39.15*	60.00 50.85*	16.67 23.86*	36.67 37.14*	73.33 59.01*	100.00 90.00*	100.00 90.00*	70.00 61.92*	86.67 72.79*	100.00 90.00*	100.00 90.00*	100.00 90.00*
T ₄	0.00 0.00*	16.67 23.86*	33.33 35.22*	60.00 50.85*	83.33 66.15*	26.67 31.00*	50.00 45.00*	90.00 71.57*	100.00 90.00*	100.00 90.00*	60.00 50.85*	93.33 81.15*	100.00 90.00*	100.00 90.00*	100.00 90.00*
T ₅	0.00 0.00*	16.67 23.86*	46.67 43.08*	56.67 48.85*	70.00 57.00*	26.67 31.00*	53.33 46.92*	83.33 66.15*	100.00 90.00*	100.00 90.00*	63.33 52.78*	93.33 77.71*	100.00 90.00*	100.00 90.00*	100.00 90.00*
T ₆	0.00 0.00*	33.33 35.01*	66.67 54.78*	90.00 75.00*	100.00 90.00*	26.67 31.00*	63.33 52.78*	100.00 90.00*	100.00 90.00*	100.00 90.00*	86.67 76.93*	93.33 81.15*	100.00 90.00*	100.00 90.00*	100.00 90.00*
T ₇	0.00 0.00*	16.67 23.86*	33.33 35.22*	60.00 50.85*	83.33 66.15*	23.33 28.78*	53.33 46.92*	100.00 90.00*	100.00 90.00*	100.00 90.00*	90.00 75.00*	100.00 90.00*	100.00 90.00*	100.00 90.00*	100.00 90.00*
T ₈	0.00 0.00*	33.33 34.93*	63.33 53.15*	93.33 81.15*	100.00 90.00*	56.67 48.93*	93.33 77.71*	100.00 90.00*	100.00 90.00*	100.00 90.00*	96.67 83.86*	100.00 90.00*	100.00 90.00*	100.00 90.00*	100.00 90.00*

CD_{0.05} Analogs (T₁-T₂, T₃-T₈) x Concentration (ppm) x Exposure period (in hours 4.82

T₁: Pyriproxyfen (Standard); T₂: Fenoxycarb (Standard)

T₃: N-(1-isopropyl-2-anilino-2-oxo-ethyl) benzene sulphonamide; T₄: N-(1-isopropyl-2-anilino-2-oxo-ethyl) toluene- sulphonamide

T₅: N-(1-isopropyl-2- p-chloroanilino-2-oxo -ethyl) benzene-sulphonamides; T₆: N-(1-isopropyl-2- p-chloroanilino-2-oxo-ethyl) toluene-sulphonamides

T₇:N-(1-isopropyl-2-p-nitroanilino-2-oxo-ethyl)benzene-sulphonamides;T₈:N-(1-isopropyl-2-p-nitroanilino-2-oxoethyl)toluene-sulphonamides

* angular transformed values.

the number of heteroatoms/functionality groups on the aromatic moiety, etc. [67].

Docking identifies the correct position of the molecule inside the binding pocket of the receptor and also predicts affinity level between the molecule and the receptor [24,41,9,7,62,63]. AutoDock program has been applied to investigate the binding energy profile (B.E. (ΔG_b) Kcal/mol), inhibition constant (Ki in μ M) of sulfonamide series (T₃-T₈) and in use IGRs (T₁-T₂) with JHBP of *G. mellonella* (2RCK) (Fig. 3). The energy profile was sequenced according to the binding energy and inhibitory constant (Ki) (Table 4).

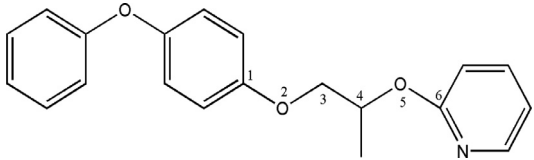
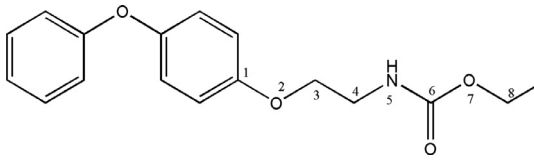
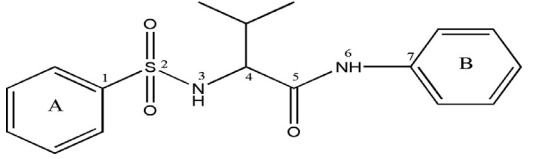
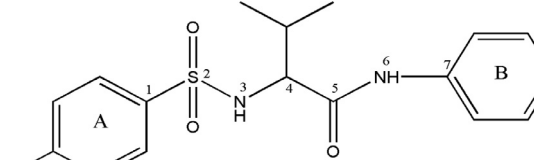
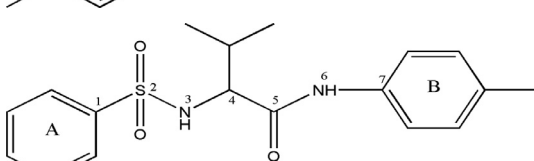
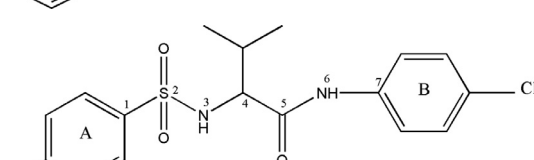
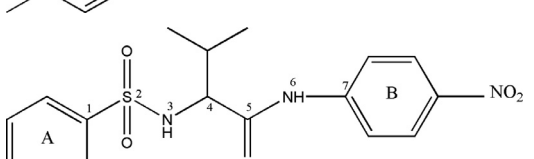
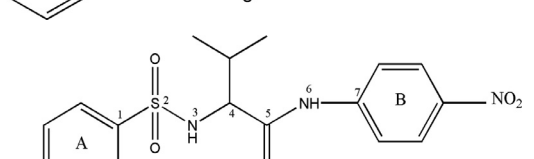
All synthesized analogs illustrate a low binding energy profile than Fenoxycarb but higher than Pyriproxyfen upon interaction with JHBP. Among synthesized analogs, analog T₈ having lower binding energy followed by T₇, T₃, T₄, T₅, and T₆ analogs, respec-

tively. Lower binding energy profile is due to the presence of two different functional groups at the terminals of the main chain. This structural deviation leads to strain at the main chain and prevents the folding of the analog inside the binding pocket of JHBP. There was a large deviation in the value of the total internal energy of synthesized sulfonamide analogs (T₃-T₈) over commercial IGRs i.e Pyriproxyfen (T₁) and Fenoxycarb (T₂) (Fig. 7(a-b)).

The fluctuating energy profile of synthesized analogs is due to the variation of substituted groups at the rings i.e., A & B (Table 4). Torsional energy is associated with the degree of freedom of the molecule and more is the degree of freedom larger will be the possibility of change in the conformation inside the pocket. The polar-NO₂ group in analogs T₇-T₈ exhibited a lowering in binding energy profile. As olfactory sensations of the insects require some degree

Table 4

Free energy of binding (ΔG_b , Kcal/mol), Inhibitory constant (K_i in μM) and Hydrogen bond interactions along with distances (\AA) of IGRs (in use T_1 - T_2 and synthesized T_3 - T_8) with JHBP of *G. mellonella*

S. No.	IDs	Ligands	InhibitionConst Energy (Kcal/mol)	Binding Energy Torsional energy (Kcal/mol)	Docking Ki(μM^* , nM **) (Kcal/mol)	Binding interactions	Distances (\AA)	Number in Cluster	
1.	T_1		5.32*	-7.18	-8.25	0.60	O ₂OH THR 22 O ₅OH THR 22	2.781 2.587	99
2.	T_2		136.43*	-5.27	-0.69	1.19	O ₆HN LYS 218	1.779	42
3.	T_3		3.35*	-7.74	-10.3	1.79	O ₅NH LYS 218 NH ₆OH THR 22	2.019 2.119	28
4.	T_4		7.03*	-7.03	-10.04	1.79	O-S- O.....NH LYS 218 NH ₆OH THR 22	1.879 2.001	27
5.	T_5		7.98*	-6.96	-10.04	1.79	O ₅HN LYS 218 NH ₆OH THR 22	2.002 2.096	2
6.	T_6		21.02*	-6.38	-9.47	1.79	OSO.....HN LYS 218 NH ₃OH THR 22	1.669 2.131	3
7.	T_7		1.23*	-8.06	-11.25	2.09	OSO....HN LYS 218 ONO.....HN LYS 85	1.976 1.706	17
8.	T_8		941.82**	-8.22	-11.61	2.09	NH ₆OH TYR 130 ONO----HN LYS 85	1.931 1.701	24

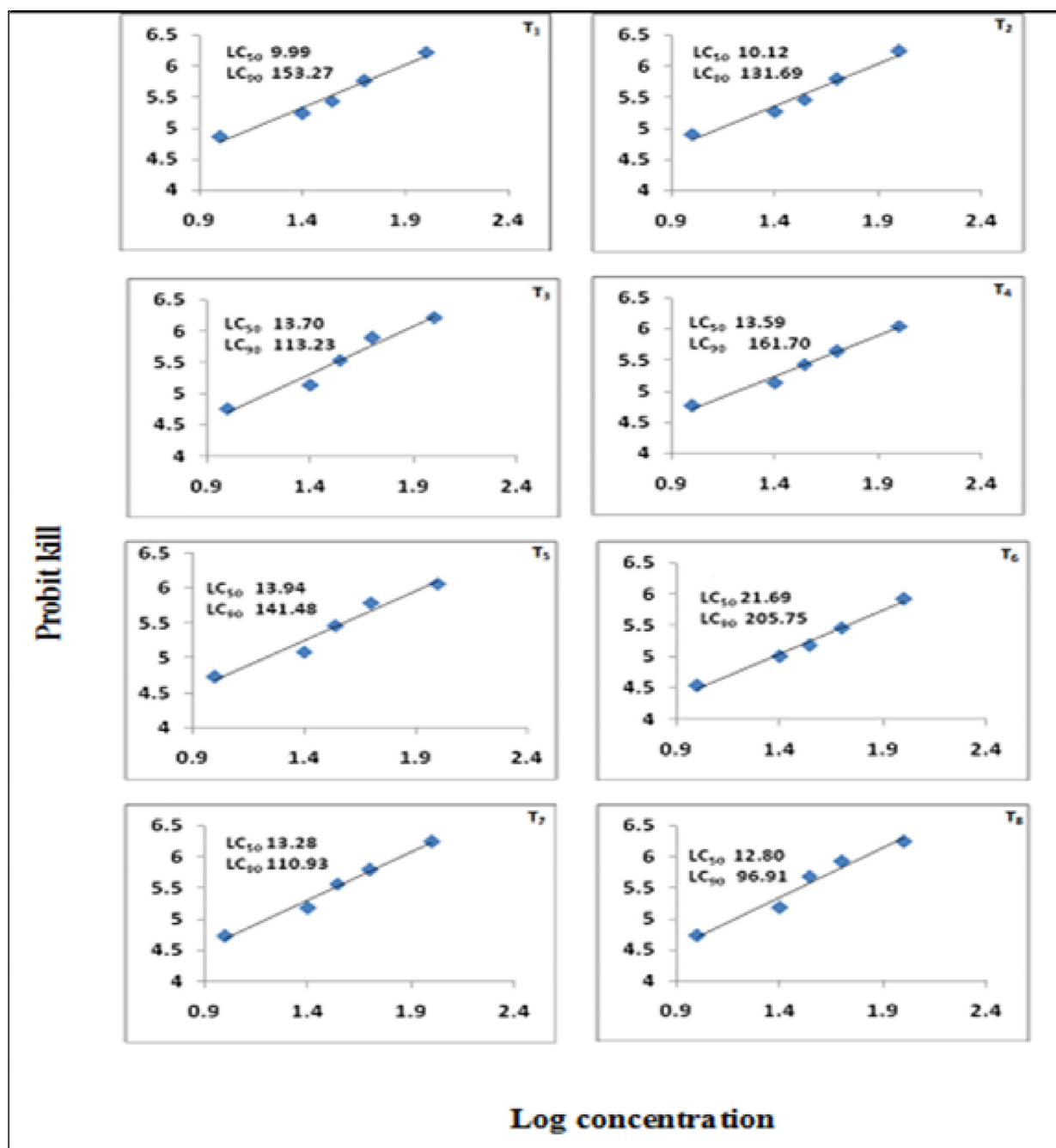


Fig. 4. Concentration-mortality response of different analogs to fourth-instar larvae of *G. mellonella* by topical application method.

of lipid solubility, therefore, hydrophobicity/lipophilicity of the repellents is likely to be an important factor for potent repellent activity [35,60,39,42,18,78]. Inhibitory constant (Ki) likewise as B.E. profile for all the synthetic analogs, and in use IGRs (T₁-T₂). Synthesized analogs T₈, T₇, and T₃ possess lower value for inhibitory constant (Ki) in comparison to the rest of the analogs (Table 4). The values of inhibition constant of these synthetic analogs are comparable to Pyriproxyfen (T₁).

Synthetic IGR, Pyriproxyfen (T₁) having a functional group at 2nd and 5th position showed H-bonding with THR 22. The pyridine ring being hydrophobic moiety showed additional H-bond interactions with PRO 146 amino acid residue of the pocket (Fig. 8).

In Fenoxycarb (T₂), the group at the 6th position formed H-bonding with LYS 218. It also showed additional interactions with THR22, TYR 130 which could be the reason for their good bind-

ing energy behavior over synthesized analogs with JHBP of *G. mellonella* (Fig. 8).

Analog T₇ and T₈ having -NO₂ group at the para position to ring B, forming H-bond with pocket residues THR 22, LYS 85, 218 and TYR 130 (Table 4) adopts an extended conformation inside the binding cavity with a decrease in binding energy in comparison to T₅ and T₆ analogs with p-substituted Cl group. Closer the packing of the analogs stronger will be the JHAs - JHBP complex and effective will be the interactions with decreased binding energy. Therefore, it is concluded that functionalities present at position 2nd, 5th, and 6th interact effectively via H-bonding with amino acid residues inside the binding pocket. (Fig. 8).

Synthesized analogs showed additional H-bond interactions with amino acid residues- CYS 10, ALA 21, 220, PRO146, SER129, HIS 207, ARG 210, 214 at the binding pocket which confirms

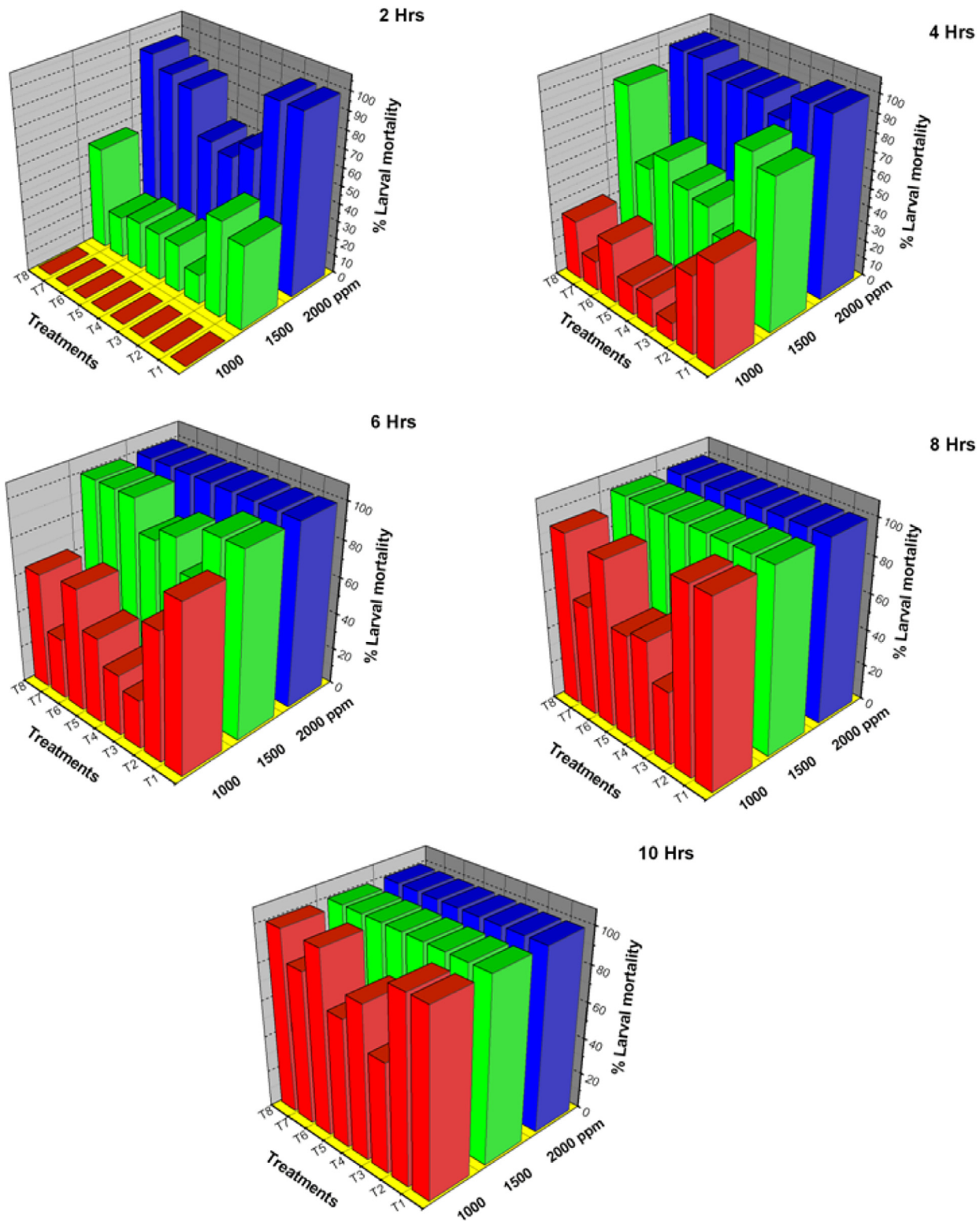
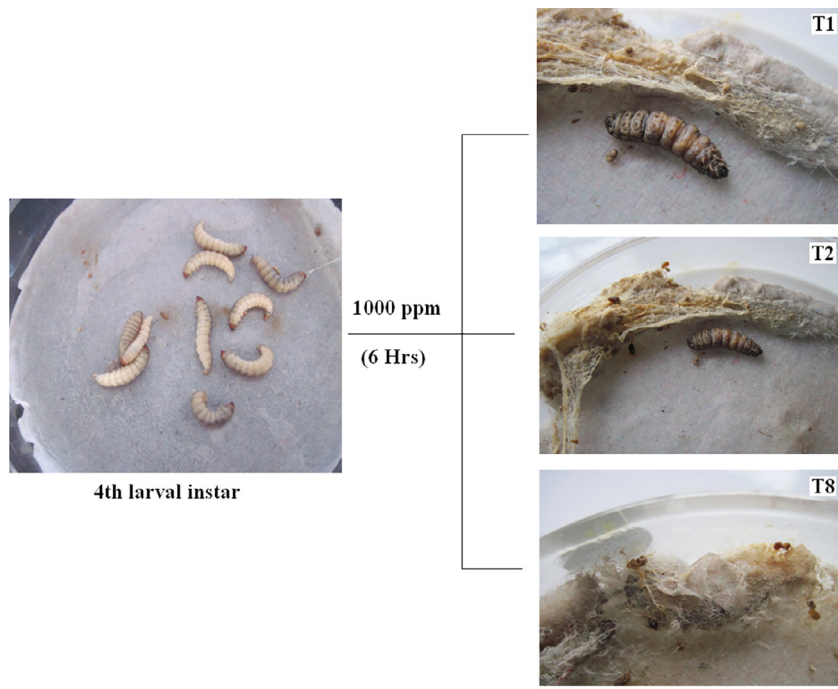
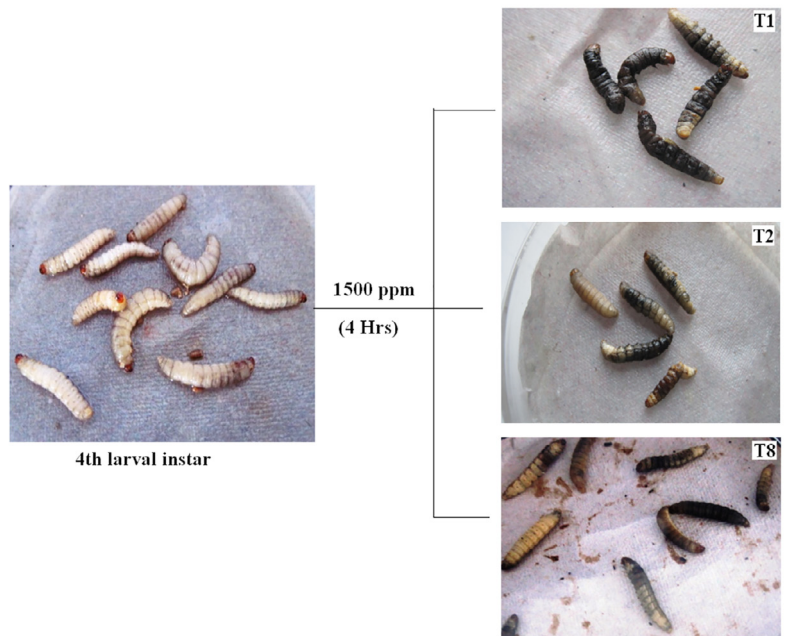


Fig. 5. Effect of different concentration (in ppm) at different exposure period (in Hours) on percent larval mortality of *G. mellonella*



a



b

Fig. 6. (a) Physiological changes on *G. mellonella* larvae after applying 1000 ppm concentrations of N-(1-isopropyl -2- p-nitroanilino-2-oxo ethyl)-p-toluene sulfonamide (T₈) at exposure period of 6 hrs. in comparison to Pyriproxyfen (T₁) and Fenoxycarb (T₂); (b); Physiological changes on *G. mellonella* larvae after applying 1500 ppm concentrations of N-(1-isopropyl -2- p-nitroanilino-2-oxo ethyl)-p-toluene sulfonamide (T₈) at exposure period of 4 hrs. in comparison to Pyriproxyfen (T₁) and Fenoxycarb (T₂); (c): Physiological changes on *G. mellonella* larvae after applying 2000 ppm concentrations of N-(1-isopropyl -2- p-nitroanilino-2-oxo ethyl)-p-toluene sulfonamide (T₈) at exposure period of 2 hrs. in comparison to Pyriproxyfen (T₁) and Fenoxycarb (T₂);

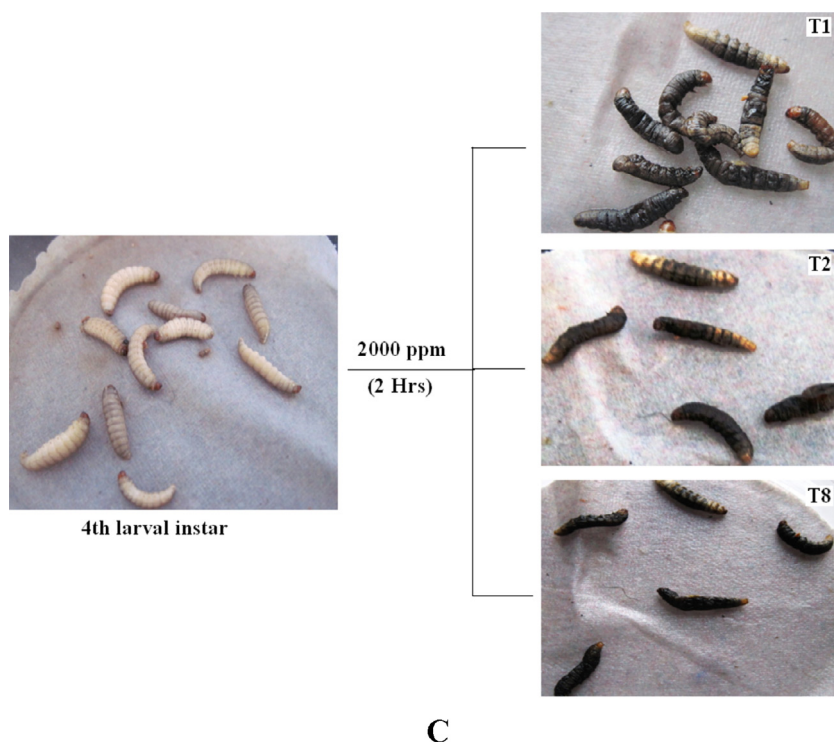


Fig. 6. Continued

Table 5

Additional interactions (bold – common, normal- additional) of the IGRs (in use T₁-T₂ and synthesized T₃-T₈) with amino acid residues at the binding pocket of JHBP of *G. mellonella*

S.No.	IDs	Additional Interactions of the ligands with amino acid residues inside the binding pocket
1.	T ₁	THR 22, LYS 85,218 , PRO** 146**, THR 148
2.	T ₂	THR 22, TYR 130, LYS 218
3.	T ₃	ALA 21, THR22 , HIS* 207, ARG** 210-214, SER* 129, TYR 130 , PRO** 146, GLU 147, THR 148, LYS 218
4.	T ₄	ILE 18, ALA, THR 22 , SER* 129, TYR 130 , PRO** 146, GLU 147, THR 148, HIS* 207, ARG** 210, LYS 218, ALA21, 220
5.	T ₅	CYS10, THR22 , ASN 94, TYR 130 , TYR142, LYS 218, ALA220
6.	T ₆	CYS10, ALA 21, THR22, TYR 130, LYS 92, 218, ALA 220 ,
7.	T ₇	ALA 21, THR 22, LYS 39,85, 133,218 TYR 130 , GLU 147, HIS* 207, ARG** 210,214, ALA220
8.	T ₈	THR 22, LYS 39,85,133,218, TYR 130 , GLU 147, ALA21,220, HIS* 207, ARG** 210, 214

* Mixed codon

** Strong codon,

the hydrophobic, acidic, and basic nature of the binding pocket (Table 5). The amino acid moieties having additional interactions are referred to as the strong codon for effective binding. They had shown a strong tendency to form H-Bond with JH analogs [73]. These simulation results corroborate with the spectroscopic studies of the binding of JH-II with JHBP of *G. mellonella* [47].

The addition of the aromatic ring at one terminal increased the hydrophobic character of the analog hence enhanced π – cation interactions which stabilize the analogs inside the pocket (Fig. 8). Docking studies have shown that more/increased would be the hydrophobic character in JH analogs; more will be the activity in terms of binding energy profile [7,62,63].

3.4. ADMET Prediction

It is of utmost importance to design and develop effective insecticide and pesticide, however, these chemicals should not be toxic to the environment and living organisms. As the direct animal test is time-consuming, therefore, in silico model based on the structure-activity relationship (SAR) obtained from past knowledge could be very useful in predicting the toxic effect of synthesized JH analogs. It is important to predict toxicity before the development/ launch of the chemical/drug for any application. Therefore, to predict the side effects of new candidate compounds, ADMET simulation proved to be one of the most effective methods.

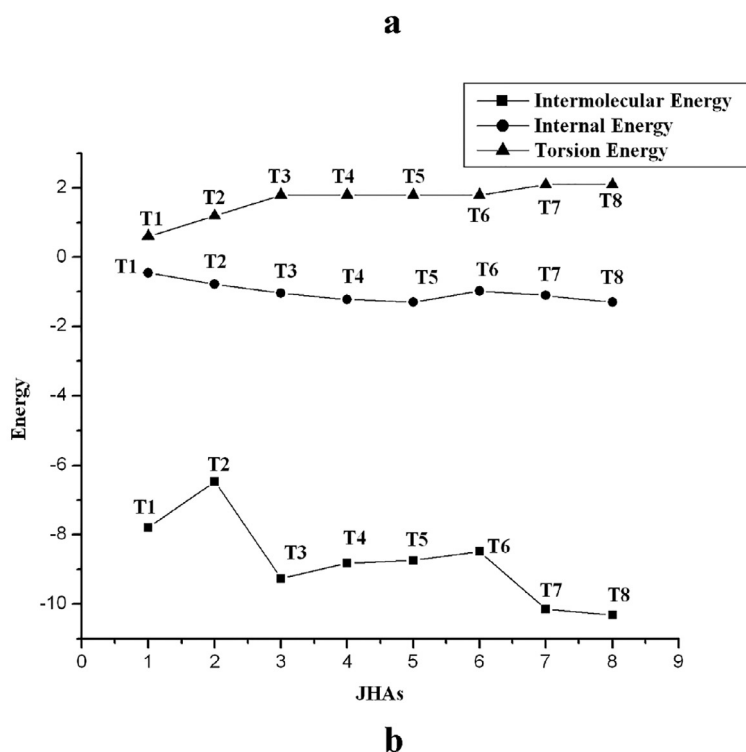
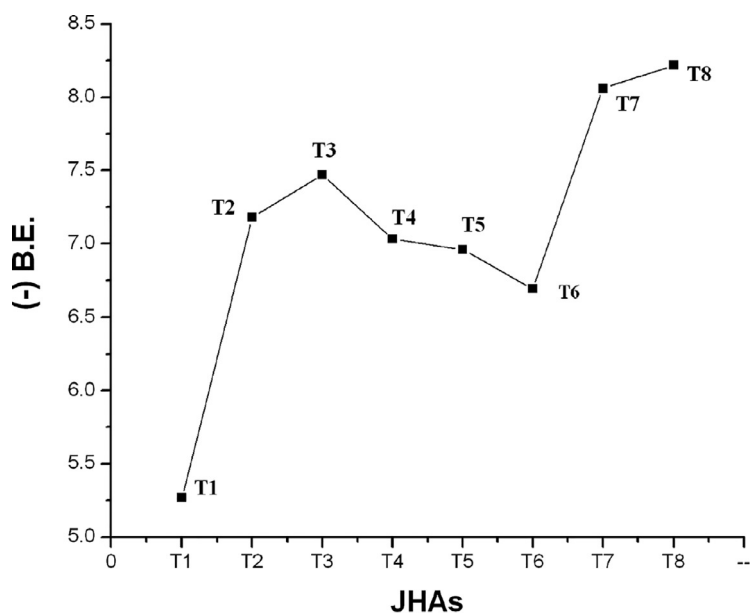


Fig. 7. (a) Binding energy profile of IGRs (T₁-T₈); (b): Energy variations (intermolecular, internal and torsional energy) of all the analogues with juvenile hormone binding protein of *G. mellonella*.

ADMET predictions were carried out to evaluate the drug-likeness of sulfonamide analogs and the properties were reported in table 6 along with biplot Fig. 9.

The pharmacokinetic profile of analogs was predicted using six precalculated ADMET models provided by Discovery Studio. Fig. 9 biplot shows two analogs 95 % and 99% confidence ellipse corresponding to HIA and BBB models. PSA has an inverse relationship with human intestinal absorption and thus cell wall permeability. ADMET_BBB (Blood-Brain Barrier) predicts the blood-brain penetration power of analogs after oral administration. The values of BBB level for (T₁-T₂) coming out to be 0 and 1 indicates a high BB penetration level whereas in the case of synthesized JH analogs (T₃-T₈) values come to be 2 i.e. medium penetration level.

ADMET_PPBB (Plasma Protein Binding) shows the extent of binding of analogs (T₁-T₈) with the carrier protein is greater than 2 corresponds to binding greater than 95%. The aqueous solubility of the analogs is low to optimal indicates bioavailability. The value of the absorption level for all (T₁-T₈) analogs corresponds to value 2 indicates low intestine absorption. ADMET_CYP2D6 values predict the non-inhibitor nature of analogs in the human system. The value of CYP_2D6 is less than even zero. All the analogs having zero and negative CYP_2D6 values indicate their non-toxic nature. ADMET Hepatotoxic data indicates the non-toxic nature of all the analogs (T₁-T₈) to the liver. The Log P is used to estimate the lipophilicity, thus the information of H-bonding characteristics as

Table 6ADMET prediction of in use IGRs (T₁-T₂) and synthesized JHAs (T₃-T₈):

Analogs	AlogP	PSA_2D	PPB	Hepatotoxicity	CYP2D6 binding	Aqueous solubility	BBB penetration	Intestinal absorption
T ₁	4.6	20.19	True(highly bounded)	False(non-toxic)	False(non-inhibitor)	2(low)	0(very good)	0(good)
T ₂	3.2	47.97	True(highly bounded)	False(non-toxic)	False(non-inhibitor)	3(good)	1(good)	0(good)
T ₃	2.7	77.52	True(highly bounded)	False(non-toxic)	False(non-inhibitor)	3(good)	2(medium)	0(good)
T ₄	3.1	77.52	True(highly bounded)	False(non-toxic)	False(non-inhibitor)	2(low)	2(medium)	0(good)
T ₅	3.3	77.52	True(highly bounded)	False(non-toxic)	False(non-inhibitor)	2(low)	2(medium)	0(good)
T ₆	3.8	77.52	True(highly bounded)	False(non-toxic)	False(non-inhibitor)	2(low)	2(medium)	0(good)
T ₇	2.5	120.34	True(highly bounded)	False(non-toxic)	False(non-inhibitor)	2(low)	2(medium)	0(good)
T ₈	3.0	120.34	True(highly bounded)	False(non-toxic)	False(non-inhibitor)	2(low)	2(medium)	0(good)

Abbreviations: AlogP, the logarithm of the partition coefficient between n-octanol and water; PSA, polar surface area, CYP450 cytochrome P450, PPB plasma protein binding, BBB blood-brain barrier

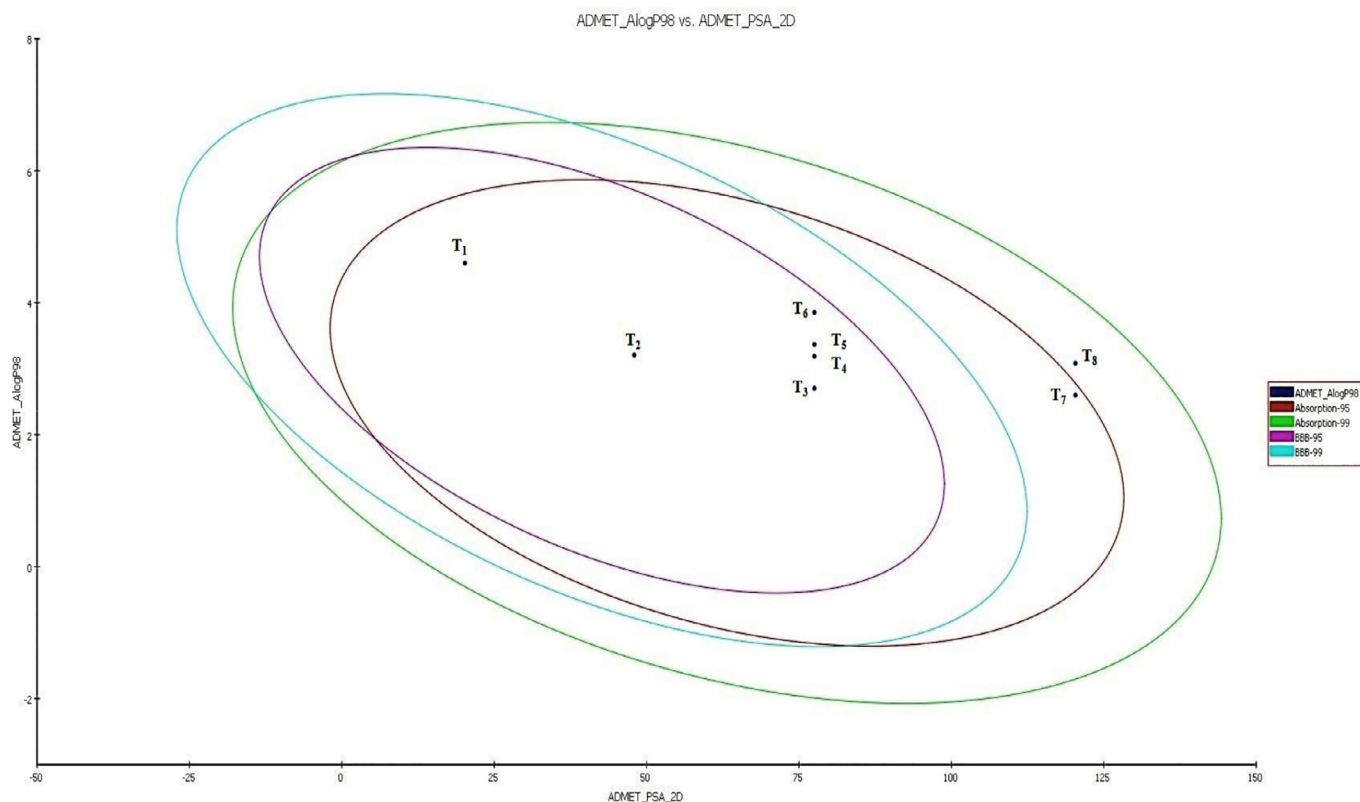


Fig. 9. Prediction of analogs absorption for various PA considered for IGR activity. Discovery Studio 2.1 (Accelrys, San Diego, CA) ADMET Descriptors, 2D polar surface area (PSA_2D) in Å² for each analog is plotted against their corresponding calculated atom-type partition coefficient (Alog98). The area encompassed by the ellipse is a prediction of good absorption with no violation of ADMET properties. The plot of Polar Surface Area (PSA) vs. LogP for a standard and test set showing the 95% and 99% confidence limit ellipse corresponding to the Blood-Brain Barrier and Intestinal Absorption models.

Table 7Toxicity prediction of synthetic IGRs (T₁&T₂) and JH analogs (T₃-T₈):

Analogs	Topkat mouse female *NTP prediction	Topkat mouse male *NTP prediction	Mouse female #fda	Mouse male FDA	Topkat skin irritancy
T ₁	NC	NC	NC	NC	None
T ₂	NC	NC	NC	NC	None
T ₃	NC	NC	NC	NC	None
T ₄	NC	NC	NC	NC	None
T ₅	NC	NC	NC	NC	None
T ₆	NC	NC	NC	NC	None
T ₇	NC	NC	NC	NC	None
T ₈	NC	NC	NC	NC	None

*NTP – National Toxicology Predictions, #fda- food and drug administration, NC- Non-Carcinogen

a small frontier orbital gap is more polarizable and is generally associated with a high chemical reactivity, low kinetic stability, and is also termed as a soft molecule [72,26,55,56]. The HOMO and LUMO energies are used as chemical reactivity ratios and are usually associated with other indexes such as electron affinity and ion-

ization potential. The energy of HOMO is directly related to the ionization potential and LUMO energy is directly related to the electron affinity. The energy difference between HOMO and LUMO orbitals is called as energy gap which serves as an important stability factor for the proposed analogs.

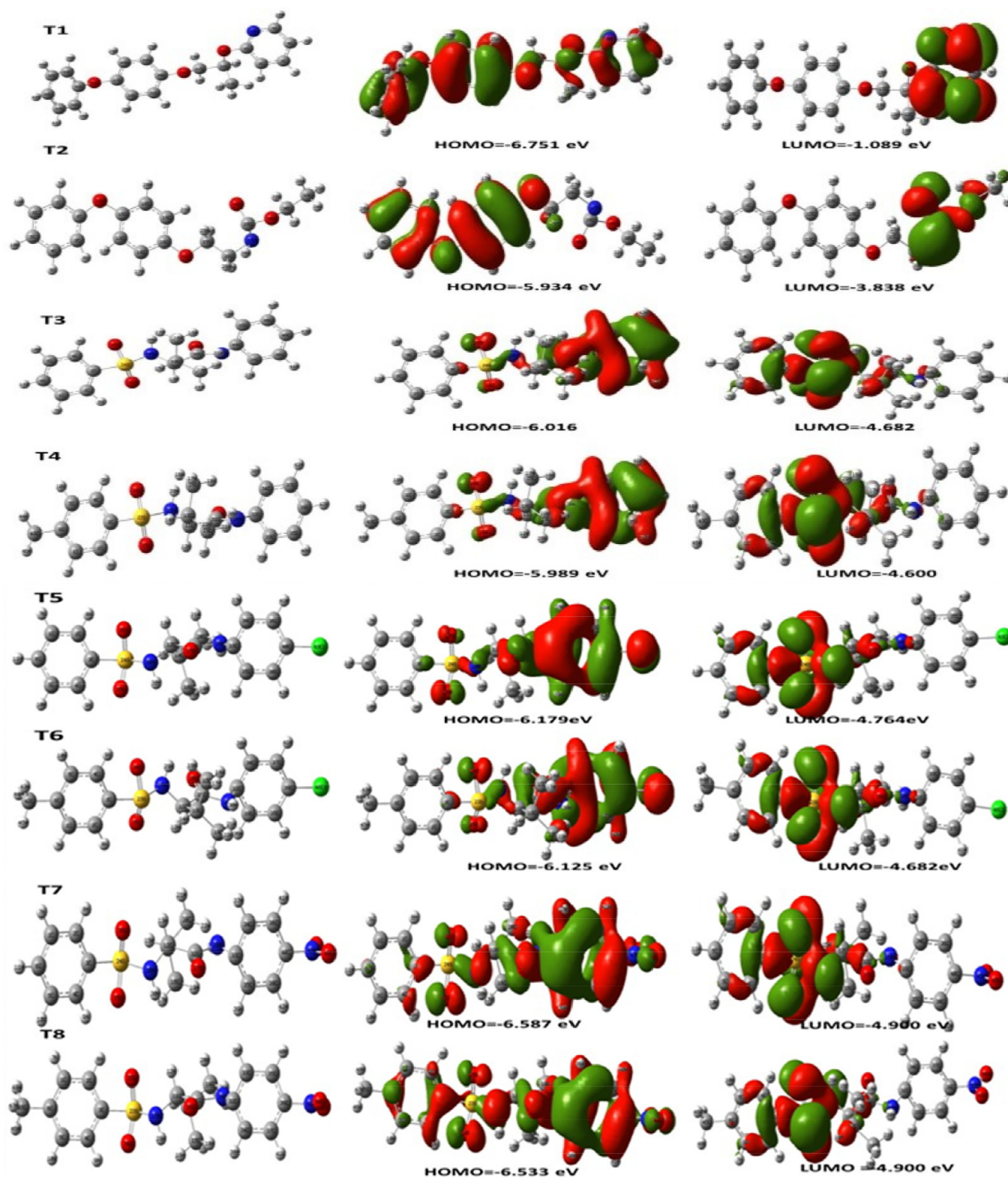


Fig. 10. Graphical view of DFT originated wavefunctions (molecular orbitals) in the form of HOMO-LUMO orbitals from occupied and virtual molecular orbitals of titled analogs (T₁-T₈) visualized by Gaussview 3.0. Red and green color distribution represents positive and negative phase in molecular orbital wave function, respectively.

The HOMO-LUMO energy gap for the analogs T₈ and T₇ is 1.6 eV which confirms that the proposed analogs have a stable structure. The lower the energy gap, the more easily electrons are excited from the ground state to the excited state (Fig. 10, Table 8).

3.6. Global Reactivity Descriptors

Global reactivity descriptors act as a bridge between the stability of the structures and global chemical reactivity. Based on frontier molecular orbital (FMO) energies the global reactivity descrip-

Table 8

The HOMO and LUMO energies and the energy gap between HOMO and LUMO (ΔE_g) in eV units at DFT/6-31+G (d, p) level in the gas phase

S.No	Analog	HOMO (in eV)	LUMO (in eV)	Energy Gap (ΔE_g in eV)
1.	T ₁	-6.751	-1.089	-5.662
2.	T ₂	-5.934	-3.838	-2.096
3.	T ₃	-6.016	-4.682	-1.334
4.	T ₄	-5.989	-4.600	-1.388
5.	T ₅	-6.179	-4.764	-1.415
6.	T ₆	-6.125	-4.682	-1.443
7.	T ₇	-6.587	-4.900	-1.688
8.	T ₈	-6.533	-4.900	-1.633

tors such as electronegativity (χ), chemical potential (μ), global hardness (η), global softness (S), and global electrophilicity index (ω) have been calculated for aniline based sulfonamide analogs (T₃-T₈) along with in-use IGRs (T₁-T₂) (Table 9). The concept of these parameters is related to each other:

$$\text{Chemical potential } (\mu) = \frac{1}{2}(E_{\text{LUMO}} + E_{\text{HOMO}})$$

$$\text{Electronegativity } (\chi) = -\mu = -\frac{1}{2}(E_{\text{LUMO}} + E_{\text{HOMO}})$$

$$\text{Global Hardness } (\eta) = \frac{1}{2}(E_{\text{LUMO}} - E_{\text{HOMO}})$$

$$\text{Softness } (S) = 1/\eta$$

$$\text{Electrophilicity } (\omega) = \mu^2/2\eta$$

The electrophilicity index helps in describing the biological activity of the proposed analogs (T₃-T₈). Considering the chemical hardness, a large HOMO-LUMO gap means- a hard molecule (more stable & less reactive), and small HOMO-LUMO means -a soft molecule. One can also relate the stability of the analog with the least energy gap which is related to high reactivity. The analogs T₇ and T₈ have the lowest energy gap ($E_{\text{gap}} = 1.60$ eV) and this lower energy gap makes the analog soft. The analog T₄ has the highest HOMO energy ($E_{\text{HOMO}} = -5.989$ eV) known to the best electron donor. The analog T₈ has the lowest LUMO energy ($E_{\text{LUMO}} = -4.900$ eV) which signifies that it can be the best electron acceptor. The two properties like I (potential ionization) and A (affinity) can be used to calculate the absolute electronegativity and the absolute hardness. These two parameters are related to the one-electron orbital energies of the HOMO and LUMO respectively. Analog T₄ has the lowest value of the potential ionization ($I = 5.989$ eV), so that will be the better electron donor. Analog T₈ has the largest value of the affinity ($A = 4.900$ eV), so it is the better electron acceptor. The chemical reactivity varies with the structure of molecules. Electronegativity and chemical hardness help to predict the formation of the chemical bonds and the physical, chemical properties of the analogs. Chemical hardness is related to the stability and reactivity of a chemical system, it measures the resistance to change in the electron distribution or charge transfer. Chemical hardness (softness) value of analog T₃ ($\eta = 0.6670$ eV, $S = 1.499$ eV) is lesser (greater) among all the analogs (T₁-T₈). Thus, analog T₃ is found to be more reactive than all the analogs T₁-T₈. Analog T₇ & T₈ possess higher electronegativity value ($\chi = 5.7$ eV) than rest, hence; it is the best electron acceptor. The electrophilicity index (ω) measures the propensity or capacity of a species to accept electrons. The value of ω for T₃ ($\omega = 21.448$ eV) indicates that it is the stronger nucleophile whereas analog T₇ is the strongest electrophiles among all analogs. Analog T₇ & T₈ have the smaller frontier orbital gap so, are more polarizable and associated with a high chemical reactivity, low kinetic stability, and termed as a soft analog. Ionization energy is a fundamental descriptor of the chemical reactivity of atoms and molecules. High ionization energy indicates high stability and chemical inertness, and small ionization energy indicates high reactivity of the atoms and molecules. Absolute hardness and softness are important properties to measure molecular stability and reactivity. It is apparent that the chemical hardness fundamentally signifies the resistance towards the defor-

Table 9 Calculated Global Quantities ionization potential (I), electron affinity (A), Chemical potential (μ), Electronegativity (χ), Hardness (η), Softness (S), and Electrophilicity (ω) of different analogs (T₁-T₈) eV at DFT/6-31+G (d, p) level in gas phase.

S. No	Ionization enthalpy (I)	Electron affinity (A)	Chemical Hardness (η)	Chemical Potential (μ)	Softness (S)	Electrophilicity (ω)	Electrophilicity (v)	Nucleophilicity (χ)	Electronegativity (χ)	Charge Transfer (I)	Nucleo fugality ΔE_N	Electro fugality ΔE_E	Dipole Moment (D)
T ₁	6.751	1.089	2.831	-3.920	0.353	2.714	0.3685	3.920	3.920	1.38	0.210	8.050	3.50
T ₂	5.934	3.838	1.048	-4.886	0.954	11.390	0.0878	4.886	4.886	4.66	7.028	16.800	3.03
T ₃	6.016	4.682	0.667	-5.349	1.499	21.448	0.0466	5.349	5.349	8.02	16.433	27.131	5.33
T ₄	5.989	4.600	0.695	-5.295	1.440	20.181	0.0496	5.295	5.295	7.63	15.234	25.823	5.18
T ₅	6.179	4.764	0.708	-5.472	1.413	21.157	0.0473	5.472	5.472	7.73	16.039	26.982	5.34
T ₆	6.125	4.682	0.722	-5.404	1.386	20.234	0.0494	5.404	5.404	7.49	15.191	25.998	5.49
T ₇	6.587	4.900	0.844	-5.744	1.186	19.554	0.0511	5.744	5.744	6.80	14.232	25.749	6.84
T ₈	6.533	4.900	0.817	-5.717	1.224	20.011	0.0500	5.717	5.717	6.80	14.703	26.136	7.29

mation or polarization of the electron cloud of the atoms, ions, or molecules under small perturbation of chemical reaction.

Conclusions

The proposed work is a part of a synthesis, *in vivo* efficacy, docking, ADMET, and Frontier Molecular Orbital analysis of effective and environmentally safe JH analogs to be Insect Growth Regulators (IGRs). We have synthesized series of analogs containing activating groups like sulfur, L-amino acids, (un) substituted aniline derivatives. Sulfur being the essential nutrients to the plants also plays an important role in chlorophyll during photosynthesis and showed important role in agrochemicals. Sulfur-containing compounds are biodegradable finds a unique place in the Pharmaceutical and pesticidal industry [21]. Sulfonamide functionality, aniline bearing - chloro/ nitro group at the para position are the key factors for the enhanced bioactivity of the analogs in comparison to in use IGRs (T₁ & T₂) [35,39,42,18,78]. *In Vivo* Evaluation of T₃-T₈ along with commercial IGRs T₁&T₂, on *G. mellonella* has been carried out with diverse concentrations (in ppm) with the varied exposure time (in hours). The general picture of sulfonamide formulations used in this study could be rated as T₈ > T₇ > T₆ > T₃ > T₅ > T₄ i.e. in decreasing order of their effectiveness against *G. mellonella*.

Virtual screening of all the analogs (T₁-T₈) has been performed using JHBP (2RCK) of *G. mellonella* on AutoDock 4.2 software. Molecular docking suggests that juvenile hormone analogs with minimum binding energy will fit better inside the binding pocket of the receptor protein [46]. Six synthetic analogs reported in this paper differ from one another based on substituent groups attached at aromatic ring A and B. Synthesized JHAs (T₃-T₈) bears lower binding energy profile as compared to Fenoxycarb (IGRs), but higher than Pyriproxyfen (IGRs). Among synthesized series (T₃-T₈); analog T₈ bears the lowest energy profile followed by T₇ and T₃ analogs. Methylated analogs (T₈) having nitro functionality at the para-position of aromatic B ring results in the lowest binding energy in comparison to the chloro analogs. Some inter or intratomic interactions are induced by -NO₂ group substitution at para- position of ring B which further believes to affect the binding mode. Overall, the study confirms that all synthesized analogs (T₃-T₈) showed binding energy in the range of $\Delta G^{\circ} \geq 2\text{kcal/mol}$ hence proposed to be effective IGRs in comparison to in use (T₁ & T₂) IGRs. This study has shown the hydrophobic nature of the binding

pocket of the JH receptor protein as well as the hydrophobic nature of JHA's played a vital role in the binding process. The study also revealed that the most active compounds must possess an active atom (O/N) in the molecules. The presence of an Electron withdrawing moiety is essential for high activity [61].

Quantum chemical descriptors calculated by the density functional theory (DFT) method were used for establishing the structure-activity relationship between descriptors and bioactivity. Electrophilicity index, polarity, chemical softness, or hardness are most likely responsible for their effectiveness as good IGRs. Further, all the analogs were also tested for their toxicity prediction using the ADMET tool executed in the discovery studio software. Outcomes from ADMET analysis were compared with the standard JH analogs (IGRs T₁ & T₂) which already proved to be non-toxic in the literature, confirms the eco-friendly and biodegradable nature of compounds. Interestingly, the results of bioassay on *G. mellonella* are supported by computational results, both by docking and DFT study. A comparison between bioassay and virtual screening has been drawn in figure 11.

The theoretical trend for binding energy followed the pattern: T₈>T₇>T₃>T₁>T₄>T₅>T₆>T₂. The binding energy values for all the analogs occurred within the range of 2kcal/mol. The docking study clearly showed the similar behavior of synthesized analogs in comparison to in use IGRs (T₁ & T₂) against JHBP of *G. mellonella*. These results were further augmented by *in vivo* findings. Analog T₇ & T₈ at 2000 ppm at 4 h of exposure period showed a similar activity like that of T₁ and T₂ by yielding 100 % mortality. Further decreasing concentration to 1500 ppm at 6 hrs. exposure period; 100 % mortality has been achieved by T₆, T₇ & T₈ analogs. Thus, analog T₈ having leading behavior over T₁&T₂ as per *in vivo* study. Interestingly, bioassay results are being supported by the theoretical outcome (Fig. 11).

The incorporation of different functionalities at the main skeleton dictates the binding pattern of JH to a receptor protein (JHBP). The number of JH analogs have been synthesized and evaluated on these lines. We have incorporated different design features that are very common in other bio-applications like- sulfonamide, amide in the main chain, and incorporation of hydrophobic moieties at the three sides of the molecules (Fig. 1c). Comparing this series (T₃-T₈) with previously reported heterocyclic and aza based sulfonamide Juvabione series, [7,62,63], the addition of sulfonamide functionality at the main chain skeleton, the aromatic substitution at A & B ring, increase in hydrophobicity at the main chain, initi-

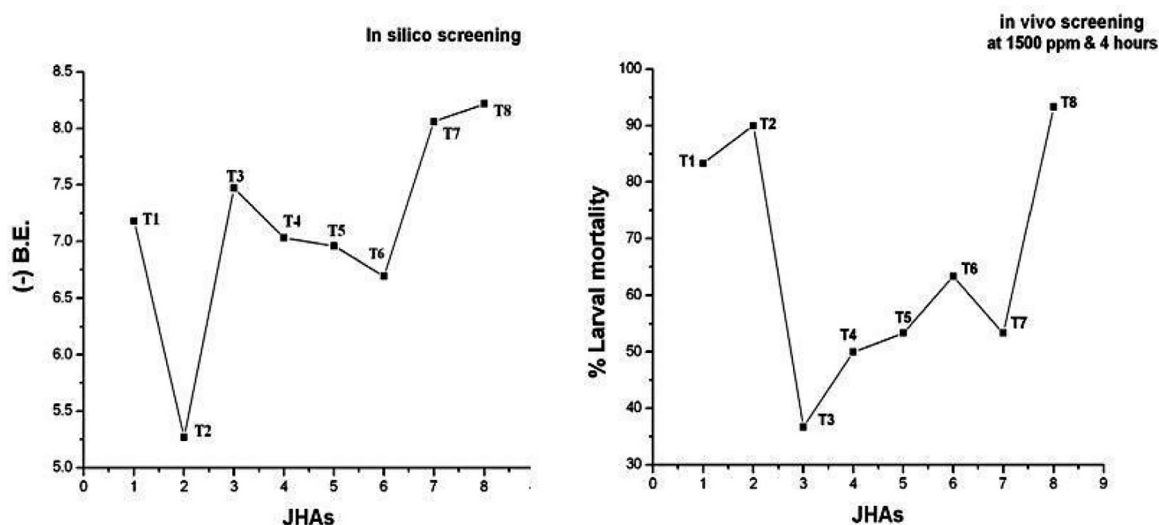


Fig. 11. Comparison of *in silico* study and *in vivo* screening (at 1500 ppm for 4 hrs.)

ates/stabilizes the ligand-receptor protein complex. The hydrophobic region of different synthesized analogs tends to come together to have an effective contribution to binding free energy (Fig. 1c). The present analysis also proposes the flexible behavior of the synthesized analogs in the Pharmaceutical industry in addition to the agrochemical industry. The combined bioassay and *in silico* study of JHAs has revealed important structural features necessary for specific interactions that these Juvenoids exhibit with JHBP of the receptor protein. The present study indicates that these JH analogs (mimics of JH) could serve as the basis for future design to find new derivatives with multiple activities to counteract lepidopteran insect species. We are in progress on the detailed investigation on lead compounds (T₇, T₈) and their environmental impact, which will be published in due course of time.

Declaration of Competing Interest

The authors declare that there is no conflict of interests regarding the publication of this paper.

Acknowledgment

The authors thank the Sophisticated Analytical Instrument Facility, Punjab University, Chandigarh, for recording FT-IR, NMR (¹H and ¹³C), and mass spectra. We are also thankful to the Director, Institute of Biotechnology, and Environmental Science- Neri (Hamirpur) H.P for extending all help in performing biological studies.. One of the authors Priyanka Sharma acknowledges MHRD, Government of India for a Ph.D. fellowship.

Supplementary materials

Supplementary material associated with this article can be found, in the online version, at doi:10.1016/j.molstruc.2021.129945.

References

- [1] W.S. Abbott, A method of computing the effectiveness of an insecticide, *J Eco Entomol* 18 (1925) 265–267.
- [2] A. Amiri, A.R. Bandani, A. Darvishzadeh, Effects of the Insect Growth Regulators Methoxyfenozide and Pyriproxyfen on Adult Diapause in Sunn Pest *Eurygaster integriceps* (Hemiptera: Scutelleridae), *J. Agr. Sci. Tech* 14 (2012) 1205–1218.
- [3] N. Aribi, G. Smagge, S. Lakbar, N. Soltani-Mazouni, N. Soltani, Effects of pyriproxyfen, a juvenile hormone analog, on development of the mealworm, *Tenebrio molitor*, *Pesticide Biochemistry and Physiology* 84 (2006) 55–62.
- [4] M. Ashfaq, N.K. Al-Tememi, S. Ahmed, Effect of artificial diets on some parameters of greater wax moth, *Galleria mellonella* L. under optimum conditions, *J. Agric. Res.* 43 (3) (2005) 223–228.
- [5] P. Awasthi, R.K. Mahajan, Synthesis of some sulphonamide insect Juvenile hormone-Part I, *Indian Journal of Chemistry* 47 B (2008) 1291–1297.
- [6] P. Awasthi, P. Sharma, Designing and Binding Mode Prediction of Juvenile Hormone Analogs as Potential Inhibitor for *Galleria mellonella*, *J Comput Sci Syst Biol* 6 (2013) 106–111.
- [7] P. Awasthi, P. Sharma, *In silico* screening of the Juvenile hormone analogues with juvenile hormone binding protein of *Galleria mellonella* - a docking study, SAR and QSAR in Environmental study 23 (7-8) (2012) 607–625.
- [8] P. Bebas, B. Cymborowski, M. Kazek, A.M. Polanska, Effects of larval diapause and the Juvenile hormone analog, fenoxycarb, on testis development and spermatogenesis in the wax moth, *Galleria mellonella* (Lepidoptera: Pyralidae), *Eur. J. Entomol* 115 (2018) 400–417.
- [9] D.R. Boina, M.E. Rogers, N. Wangb, L.L. Stelinski, Effect of pyriproxyfen, a Juvenile hormone mimic, on egg hatch, nymph development, adult emergence and reproduction of the Asian citrus psyllid, *Diaphorina citri* Kuwayama, *Pest Manag Sci* 66 (2010) 349–357.
- [10] L. Bortolotti, C. Porrini, A.M. Sbrenna, G. Sbrenna, Ovicidal action of Fenoxycarb on a predator, *Chrysoperla carnea* (Neurop-tera:Chrysopidae), *Appl. Entomol. Zool* 35 (2) (2000) 265–271.
- [11] H.S. Brar, G.S. Gatoria, H.S. Jhaji, B.S. Chahal, Seasonal infestation of *Galleria mellonella* and population of *Vespa orientalis* in *Apis mellifera* apiaries in Punjab, *Indian Journal of Ecology* 12 (1) (1985) 109–112.
- [12] R.P. Braun, G.R. Wyatt, Sequence of the Juvenile hormone binding protein from the hemolymph of *Locusta migratoria*, *J Biol Chem* 271 (1996) 31756–31762.
- [13] A. Cheng, S.L. Dixon, *In silico* models for the prediction of dose-dependent human hepatotoxicity, *Journal of ComputerAided Molecular Design* 17 (12) (2003) 811–823 2003.
- [14] J.D. Charriere, A. Imdorf, Protection of honey combs from wax moth damage, *Am. Bee J.* 139 (1999) 627–630.
- [15] A. Cheng, K.M. Merz, Prediction of aqueous solubility of a diverse set of compounds using quantitative structure-property relationships, *Journal of Medicinal Chemistry* 46 (17) (2003) 3572–3580.
- [16] K. Chen, Q. Liu, J.P. Ni, H.J. Zhu, Y.F. Li, Q. Wang, Synthesis, insecticidal activities and structure-activity relationship studies of novel anthranilic diamides containing pyridylpyrazole-4-carboxamide, *Pest Manag Science* 71 (11) (2015) 1503–1512.
- [17] S.L. Dixon, K.M. Merz, One-dimensional molecular representations and similarity calculations: methodology and validation, *Journal of Medicinal Chemistry* 44 (23) (2001) 3795–3809.
- [18] P. Devendar, F.G. Yang, Sulfur-Containing Agrochemicals, *Top Curr Chem* (Z) 375 (2017) 82.
- [19] W.J. Egan, G. Lauri, Prediction of intestinal permeability, *Advanced Drug Delivery Reviews* 54 (3) (2002) 273–289.
- [20] W.J. Egan, K.M. Merz, J.J. Baldwin, Prediction of drug absorption using multivariate statistics, *Journal of Medicinal Chemistry* 43 (21) (2000) 3867–3877.
- [21] E.X. Esposito, K. Baran, Kelly, et al., Docking of Sulfonamides to Carbonic Anhydrase II and IV, *Journal of Molecular Graphics and Modeling* 18 (2000) 283–289.
- [22] N.M. Fahmy, Impact of two insect growth regulators on the enhancement of oxidative stress and antioxidant efficiency of the cotton leaf worm, *Spodoptera littoralis* (Biosd.), *Egypt. Acad. J. Biolog. Sci.* 5 (1) (2012) 137–149.
- [23] E. Fazal, C.Y. Panicker, H.T. Varghese, S. Nagarajan, B.S. Sudha, J.A. War, S.K. Srivastava, B. Harikumar, P.L. Anto, Spectroscopic investigation (FT-IR, FT-Raman), HOMO-LUMO, NBO analysis and molecular docking study of 4-chlorophenyl quinoline-2-carboxylate, *Spectrochimica Acta Part A: Molecular and Biomolecular Spectroscopy* (2015), doi:10.1016/j.saa.2015.01.089.
- [24] M. Fenga, B. Tanga, H S Liang, X. Jiang, Sulfur Containing Scaffolds in Drugs: Synthesis and Application in Medicinal Chemistry, *Curr Top Med Chem* 16 (11) (2016) 1200–1216.
- [25] D.J. Finney, A statistical treatment of the sigmoid response curve, Probit analysis, 633, Cambridge University Press, London, 1971.
- [26] M. Frings, I. Thome, C. Bolm, Synthesis of chiral sulfoximine-based thioureas and their application in asymmetric organocatalysis, *Beilstein J. Org. Chem* 8 (2012) 1443–1451.
- [27] Z. Fujimoto, R. Suzuki, T. Shiotsuki, W. Tsuchiya, A. Tase, M. Momma, T. Yamazaki, Crystal Structure of Silkworm Bombyx mori JHBP in Complex With 2-Methyl-2,4-Pentanediol: Plasticity of JH- Binding Pocket and Ligand - Induced Conformational Change of the Second Cavity in JHBP, *PLoS ONE* 8 (2) (2013) e56261 doi:10.1371/journal.pone.0056261.
- [28] K.S. Ghoneim, Kh Hamadah, M.A. Tanani, Protein Disturbance in the Haemolymph and Fat Body of the Desert Locust *Schistocerca gregaria* as a Response to Certain Insect Growth Regulators, *Bull. Environ. Pharmacol. Life Sci.* 1 (7) (2012) 73–83.
- [29] W.G. Goodman, N.A. Granger, in: L.I. Gilbert, K. Latrou, S.S. Gill (Eds.), *Comprehensive Molecular Insect Science*, 3, Elsevier, Oxford, 2005, pp. 319–408.
- [30] W. Goodman, D.A. Schooley, L.I. Gilbert, Specificity of the Juvenile hormone binding protein: The geometrical isomers of Juvenile hormone I, *Biochemistry. Proc. Natl. Acad. Sci. USA.* 75 (1) (1978) 185–189.
- [31] S. Grenier, A.M. Grenier, Fenoxycarb, a fairly new insect growth regulator: are view of its effects on insects, *Ann. Appl. Biol* 12 (1993) 369–403.
- [32] A.Y. Guan, C.L. Liu, G. Huang, H.C. Li, S.L. Hao, Y. Xu, Z.N. Li, Design, Synthesis, and Structure-Activity Relationship of Novel Aniline Derivatives of Chlorothalonil, *J. Agric. Food Chem* 61 (2013) 11929–11936.
- [33] Y. He, D. Hu, M. Lv, L. Jin, J. Wu, S. Zeng, S. Yang, B. Song, Synthesis, insecticidal and antibacterial Activities of novel neonicotinoid analogs with dihydropyridine, *Chemistry Central Journal* 7 (2013) 76–82.
- [34] M. Hirano, M. Hatakoshi, H. Kawada, Pyriproxyfen and other Juvenile hormone analogues, *Review in Toxicology* 2 (1998) 357–394.
- [35] E. Jenwitheesuk, R. Samudrala, Improved prediction of HIV-1 protease-inhibitor binding energies by molecular dynamics simulations, *BMC Structural Biology* 3 (2003) 2.
- [36] P. Jeschke, The latest generation of halogen-containing pesticides, *Pest Manag Sci* 73 (2017) 1053–1066.
- [37] G. Jones, M. Wozniak, Y. Chu, et al., Juvenile hormone III-dependent conformational changes of the nuclear receptor ultraspiracle, *Insect Biochemistry and Molecular Biology* 32 (1) (2001) 33–49.
- [38] K.S. Ju, R.E. Parales, Nitroaromatic Compounds, from Synthesis to Biodegradation, *Microbiology And Molecular Biology Reviews* 74 (2) (2010) 250–272.
- [39] G.L. Kad, R. Kalra, Juvenile Hormone Analogs Active on Mosquitoes: Synthesis and Juvenile Hormonal Activity of Newly Synthesized Long Chain Alkoxy Alkyl Phenyl Ethers, *Arch. Pharm. Res.* 22 (5) (1999) 502–506.
- [40] M. Khosravi, R. Ebadi, H. Seyedoleslami, et al., Growth Disturbances and Inhibitory Effect of Pyriproxyfen and Diflubenzuron on the Greater Wax Moth (*Galleria mellonella* L.) under Different Temperatures, *Journal of Science and Technology of Agriculture and Natural Resources, Water and Soil Science* 12 (45) (2008) 297–311.
- [41] J.K. Koeppe, G.E. Kovalick, in: G. Litwack (Ed.), *Biochemical Actions of Hormones*, 13, Academic Press, Orlando, FL, 1986, pp. 265–303.
- [42] R. Kolodziejczyk, G. Bujacz, M. Jakob, et al., Insect Juvenile Hormone Binding Protein Shows Ancestral Fold Present in Human Lipid-Binding Proteins, *J Mol Biol* 377 (2008) 870–881.

- [47] D. Krzyżanowska, M. Lisowski, M. Kochman, UV- difference and CD spectroscopy studies on Juvenile hormone binding to its carrier protein, *J. Pept. Res.* 51 (1998) 96–102.
- [48] O.S. Kukovinets, T.I. Zvereva, V.G. Kasradze, M.I. Abdullina, G.A. Tolstikov, New Approach to the Synthesis of Pheromones and Juvenoids with Small Rings in the Molecule, *Chemistry for Sustainable Development* 16 (2008) 721–724.
- [49] G. Kumar, M.S. Khan, Study of the life cycle of greater wax moth (*Galleria mellonella*) under storage conditions in relation to different weather conditions, *Journal of Entomology and Zoology Studies* 6 (3) (2018) 444–447.
- [50] C.A. Kwadha, G.O. Ong'amo, P.N. Ndegwa, S.K. Raina, A.T. Fombong, The Biology and Control of the Greater Wax Moth, *Galleria mellonella*, *Insects* 8 (2017) 61–78.
- [51] T.X. Liu, T.Y. Chen, Effects of the insect growth regulator Fenoxycarb on immature *Chrysopepla rufilabris* (Neuroptera: Chrysopidae), *Fla. Entomol* 84 (4) (2001) 628–633.
- [52] M. Mojaver, A.R. Bandani, Effects of the Insect Growth Regulator Pyriproxyfen on Immature Stages of Sunn Pest, *Eurygaster Integriceps Puton* (Heteroptera: Scutelleridae), *Mun. Ent. Zool* 5 (1) (2010) 187–197.
- [53] G.M. Morris, D.S. Goodsell, R.S. Halliday, R. Huey, W.E. Hart, R.K. Belew, A.J. Olson, Automated Docking Using a Lamarckian Genetic Algorithm and Empirical Binding Free Energy Function, *J. Comput. Chem.* 19 (1998) 1639–1662.
- [54] V.N. Odinokov, O.S. Kukovinets, R.A. Zainullin, G.A. Tolstikov, The synthesis of insect Juvenile hormones and their analogs, *Russian Chemical Reviews* 61 (7) (1992) 731–762.
- [55] R.G. Parr, L.V. Szentpaly, S. Liu, Electrophilicity Index, *J. Am. Chem. Soc.* 121 (1999) 1922.
- [56] F.A. Pasha, H.K. Srivastava, P.P. Singh, Comparative QSAR study of phenol derivatives with the help of density functional theory, *Bioorganic & Medicinal Chemistry* 13 (2005) 6823–6829.
- [57] P. Ponnann, S. Gupta, M. Chopra, R. Tandon, S.A. Baghel, G. Gupta, K.A. Prasad, C.R. Rastogi, M. Bose, G.H. Raj, 2D-QSAR, Docking Studies, and In Silico ADMET Prediction of Polyphenolic Acetates as Substrates for Protein Acetyltransferase Function of Glutamine Synthetase of *Mycobacterium tuberculosis*, *Structural Biology* (2013) 373516.
- [58] W. Ritter, P. Akwatanakul, *Honey Bee Diseases and Pests: A Practical Guide*, FAO, Rome, Italy, 2006 Volume 4.
- [60] R.T. Roush, B.E. Tabashnik, *Pesticide Resistance in Arthropods*, Chapman & Hall, New York, 1990.
- [61] K. Slama, M. Romanuk, F. Sorm, *Insect Hormones and bioanalogues*, Springer Verlag, New York, 1974.
- [62] P. Sharma, S. Thakur, P. Awasthi, Synthesis, characterization, biological evaluation and docking study of heterocyclic based synthetic sulfonamides as potential pesticide against *Galleria mellonella*, *Applied Biochemistry Biotechnology* 176 (1) (2015) 125–139.
- [63] P. Sharma, S. Thakur, P. Awasthi, In silico and bio assay of Juvenile Hormone Analogues as an Insect Growth Regulator against *Galleria mellonella* (greater wax moth) – Part I, *Journal of Bio molecular Structure and Dynamics* 34 (5) (2016) 1061–1078.
- [64] B. Sezer, P. Ozalp, Effects Of Pyriproxyfen On Hemocyte Count And Morphology Of *Galleria mellonella*, *Fresenius Environmental Bulletin* 24 (2a) (2015).
- [65] B. Sezer, P. Ozalp, Combined Effects Of Pyriproxyfen And *Bacillus Thuringiensis* On Antioxidant Activity Of Hemolymph, Midgut and Fat Body of *Galleria mellonella* Larvae, *Fresenius Environmental Bulletin* 25 (5) (2016) 1660–1665.
- [66] R.G. Susnow, S.L. Dixon, Use of robust classification techniques for the prediction of human cytochrome P450 2D6 inhibition, *Journal of Chemical Information and Computer Sciences* 43 (2003) 1308–1315.
- [67] R. Suzuki, Z. Fujimoto, T. Shiotsuki, W. Tsuchiya, M. Momma, A. Tase, M. Miyazawa, T. Yamazaki, Structural mechanism of JH delivery in hemolymph by JHBP of silkworm, *Bombyx mori*, *Sci.Rep.* 1 (2011) 133–142.
- [68] H. Svobodova, H. Rysava, M. Pavlik, D. Saman, P. Drasar, Z. Wimmer, A Steroid conjugates: Synthesis and preliminary biological testing of pro-Juvenoids, *Bioorganic & Medicinal Chemistry* 18 (2010) 8194–8203.
- [69] K. Touhara, G.D. Prestwich, Binding site mapping of a photoaffinity-labeled Juvenile hormone binding protein, *Biochem Biophys Res Commun* 182 (2) (1992) 466–473.
- [70] S.A. Travis, *Manufacture and uses of the Aniline: A vast array of Processes and Products*, 2007.
- [71] M. Tsikolia, U.R. Bernier, M.R. Coy, K.C. Chalaire, J.J. Becnel, N.M. Agramonte, N. Tabanca, D.E. Wedge, G.G. Clark, K.J. Linthicuma, D.R. Swale, J.R. Bloomquist, Insecticidal, repellent and fungicidal properties of novel trifluoromethylphenyl amides, *Pesticide Biochemistry and Physiology* 107 (2013) 138–147.
- [72] R. Vijayaraj, V. Subramanian, P.K. Chattaraj, Comparison of Global Reactivity Descriptors Calculated Using Various Density Functionals: A QSAR Perspective, *J. Chem. Theory Comput* 5 (10) (2009) 2745.
- [73] T. Wilhelm, S. Nikolajewa, A New Classification Scheme of the Genetic Code, *J Mol Evol* 59 (2004) 598–605.
- [74] J.L. Williams, *Insects: Lepidoptera (moths)*, in: R. Morse, K. Flottum (Eds.), *In Honey Bee Pests, Predators, and Diseases*, AI Root Company, Medina, OH, USA, 1997, pp. 121–141.
- [75] Z. Wimmer, O. Jurcek, P. Jedlicka, R. Hanus, J. Kuldova, I. Hrdy, B. Bennettova, D. Saman, *Insect Pest Management Agents: Hormonogen Esters (Juvenogens)*, *J. Agric. Food Chem.* 55 (2007) 7387–7393.
- [76] Z. Wimmer, M. Rejzek, M. Zarevucka, J. Kuldova, I. Hrdy, V. Nemeč, M. Romanuk, A Series of Bicyclic Insect Juvenile Hormone Analogs of Czech Origin: Twenty Years of Development, *Journal of Chemical Ecology* 23 (3) (1997) 605–628.
- [77] J.R. Wisniewski, M. Kochman, Juvenile-hormone-binding protein from silk gland of *Galleria mellonella*, *Federation of European Biochemical Societies* 171 (1) (1984) 127–130.
- [78] K. Zheng, T.C. Zhang, P. Lin, Y. Han, H. Li, R. Ji, H. Zhang, 4-Nitroaniline Degradation by TiO₂ Catalyst Doping with Manganese, *Journal of Chemistry* (2015) 382376.
- [79] M. Zalewska, A. Kochman, J.P. Esteve, F. Lopez, K. Chaoui, C. Susini, A. Ozyhar, M. Kochman, Juvenile hormone-binding protein traffic - Interaction with ATP synthase and lipid transfer proteins, *Biochimica et Biophysica Acta* 1788 (2009) 1695–1705.